Metal-organic coordination frameworks based on mixed methylmalonate and 4,4′-bipiridine ligands: synthesis, crystal structure and magnetic properties†‡

Mariadel Déniz,[a] Jorge Pasán,[a] Oscar Fabelo,[ab] Laura Cañadillas-Delgado,[ab] Francesc Lloret,[c] Miguel Julve[c] and Catalina Ruiz-Pérez*[a]

Received (in Montpellier, France) 6th June 2010, Accepted 23rd August 2010
DOI: 10.1039/c0nj00436g

Five new complexes of formulae $[M_2(4,4'\text{-bpy})(Memal)_2X_2]_n$ [M = Fe(III) (**2**), Mn(II) (**3**), Co(II) (**4**), Ni(II) (**5**) and Zn(II) (**6**), and X = Cl^-/OH^- (**2**) and H_2O (**3–6**); 4,4′-bpy = 4,4′-bipyridine and Memal = methylmalonate dianion] have been synthesized by following the previously reported procedure for $[Cu_2(4,4'\text{-bpy})(Memal)_2(H_2O)_2]_n$ (**1**). Moreover, two new phases of the Cu(II)/Memal/4,4′-bpy system, namely $\{[Cu(4,4'\text{-bpy})_2][Cu(4,4'\text{-bpy})_2(Memal)(NO_3)(H_2O)]\}_n \cdot nNO_3 \cdot 3.5nH_2O$ (**7**) and $[Cu(4,4'\text{-bpy})_2(Memal)(H_2O)]_n \cdot nH_2O$ (**8**), were obtained by varying the synthetic conditions. They were all structurally characterized by single crystal X-ray diffraction, and the magnetic properties of **2–5**, **7** and **8** were investigated in the temperature range 1.9–295 K. **1–6** are isomorphous compounds whose structure consists of square grids of metal ions linked through *anti–syn* carboxylate bridges that grow in the crystallographic *ac* plane. These layers are pillared along the *b* axis by bis-monodentate 4,4′-bpy ligands to afford a $[4^46^6]$-**sqp** three-dimensional net. Ferro- (**1** and **5**) and antiferromagnetic (**2–4**) interactions between the metal ions are mediated by the carboxylate bridge in the *anti–syn* conformation, the bis-monodentate 4,4′-bpy ligand being unable to transmit a significant magnetic coupling. The values of the magnetic coupling (*J*) for **2–5** are −0.269(3), −0.225(2), −0.05 and +0.272(3) cm^{-1} respectively, the isotropic spin Hamiltonian being $\hat{H} = -J\sum_i \hat{S}_i \cdot \hat{S}_{i+1}$. Complexes **7** and **8** exhibit quite a different structure, as driven by the 4,4′-bpy groups. A square-grid of $[Cu(4,4'\text{-bpy})_2]^{2n+}{}_n$ occurs in **7**, which grows in the *ab* plane and is pillared through *anti–syn* carboxylate bridges from $[Cu(Memal)(4,4'\text{-bpy})_2(NO_3)(H_2O)]$ units along the *c* axis to build up a $[4^{12}6^3]$-**pcu** net. Analysis of the magnetic data for this compound shows an overall antiferromagnetic behaviour with the coexistence of ferro- and antiferromagnetic interactions. The structure of **8** consists of linear chains of copper(II) running along the *c* axis, where aquabis(4,4′-bipyridine)copper(II) units are connected by bis(monodentate) methylmalonate ligands. A significant intrachain antiferromagnetic interaction is observed in **8** through the extended Cu–OCCCO–Cu exchange pathway [$J = -1.38(1)$ cm^{-1}]. The assembling role of the 4,4′-bpy coligand in **1–8** and in previous malonate-containing complexes is analyzed and discussed.

Introduction

Crystal engineering of coordination polymers is of great interest because of the novel topologies of the compounds and the possibility of tuning fundamental physical properties such as magnetism and electrical conductivity.[1–3] Among the broad family of coordination polymers, malonate-containing metal(II) complexes are quite promising candidates because one can build templated molecular nanostructures from basic building units through supramolecular chemical assembly. A wide variety of interesting cooperative magnetic phenomena has been observed in such complexes, where the exchange interactions can be controlled chemically by altering the topology *via* the bridging ligands, as well as the coordination of the metal ions.[4–6] The advent of new techniques based on crystal engineering opens up new and exciting ways in which one can generate nanostructured materials that show prefixed or novel magnetic responses. This is essentially a bottom-up approach to obtain magnetic nanostructures that can exhibit technologically-relevant properties like ferromagnetism.

Although the past few years have witnessed significant advances in the synthesis of polymeric metal-organic frameworks (MOFs) of great structural diversity,[7] the number of reports on the design of functional coordination networks is

[a] *Laboratorio de Rayos X y Materiales Moleculares (MATMOL), Departamento de Física Fundamental II, Universidad de La Laguna, Av. Astrofísico Francisco Sánchez s/n, 38206 La Laguna (Tenerife), Spain. E-mail: caruiz@ull.es*
[b] *Institut Laue-Langevin, 6 rue Jules Horowitz, B.P. 156, 38042 Grenoble Cedex 9, France and Instituto de Ciencia de Materiales de Aragón, CSIC-Universidad de Zaragoza, Pedro Cerbuna 12, E-50009 Zaragoza, Spain*
[c] *ICMol/Departament de Química Inorgànica, Universitat de València, Polígono La Coma s/n, 46980 Paterna (València), Spain*
† This article is part of a themed issue on Coordination polymers: structure and function.
‡ Electronic supplementary information (ESI) available: CCDC reference numbers 787484 (**2**), 787485 (**3**), 787486 (**4**), 787487 (**6**), 779277 (**7**) and 779278 (**8**). For crystallographic data in CIF or other electronic format see DOI: 10.1039/c0nj00436g

still relatively small.[8] On the basis of our previous results in the crystal engineering of extended magnetic systems with malonate complexes,[4–6] we have focused on the rational design of metal-organic networks by using alkyl/aryl-malonate groups (Rmal) as starting ligands.

The hard conditions that are typically used in the synthesis of traditional inorganic zeolites make difficult the fine-tuning of subtle features like chemical functionality. However, the mild conditions employed in the preparation of MOFs allows systematic engineering of the desired chemical and physical properties *via* modifications of their constituent building blocks. In particular, the incorporation as spacers of rod-like bis-monodentate ligands such as 4,4′-bipyridine (4,4′-bpy) and its analogues has provided us with a large number of coordination polymers from 1D (chain or ladder-like)[9] to 2D (layers)[10] and 3D (diamond, NBO or or α-Po)[11–13] motifs.

Our first attempts concerned the phenylmalonate-(Phmal)[14] and methylmalonate-(Memal)[15] copper(II) complexes. The sheet-like polymer of formula $[Cu(Memal)(H_2O)]_n$, which exhibits intralayer ferromagnetic coupling, constitutes a good example of the potentiality of and interest in these systems. A magneto-structural study of this compound was accompanied by the pillaring of its constituent neutral layers through the pyrazine (pyz) and 4,4′-bpy molecules, leading to 3D compounds of formula $[Cu_2(pyz)(Memal)_2]_n$ and $[Cu_2(4,4'\text{-bpy})(Memal)_2(H_2O)_2]_n$ (**1**).[15a]

One of the aims of our study was to analyze the magneto-structural effects caused by the methyl substituent in methyl-malonate-containing copper(II) complexes. The extension of these studies to other first-row transition metal ions in the presence of 4,4′-bpy as co-ligand afforded the complexes of formulae $[M_2(4,4'\text{-bpy})(Memal)_2X_2]_n$ [M = Fe(III) (**2**), Mn(II) (**3**), Co(II) (**4**), Ni(II) (**5**) and Zn(II) (**6**); X = Cl^-/OH^- (**2**) and H_2O (**3–6**)]. Moreover, the new phases of the Cu(II)-Memal-4,4′-bpy ternary system, $\{[Cu(4,4'\text{-bpy})_2][Cu(4,4'\text{-bpy})_2(Memal)(NO_3)(H_2O)]\}_n{\cdot}nNO_3{\cdot}3.5nH_2O$ (**7**) and $[Cu(4,4'\text{-bpy})_2(Memal)(H_2O)]_n{\cdot}nH_2O$ (**8**), were obtained by modifying the procedure used in the preparation of compound **1**. The present report deals with the preparation and structural characterization of **2–8**, together with the variable-temperature magnetic study of **2–5**, **7** and **8**.

Experimental

Materials and methods

The hexahydrated copper(II), nickel(II) cobalt(II) and zinc(II) nitrate, and tetrahydrated iron(II) and manganese(II) chloride, salts were used as the sources of the metal ions. They were purchased from commercial sources and used without further purification. $[Cu_2(4,4'\text{-bpy})(Memal)_2(H_2O)_2]$ (**1**) was prepared as reported elsewhere.[15a] Elemental analyses (C, H, N) were performed on an EA 1108 CHNS–O microanalytical analyzer of the SEGAI service of the University of La Laguna. The value of the Fe : Cl (**2**) molar ratio (1 : 0.10) was determined by electron microscopy at the Servicios Generales de Apoyo a la Investigación (SEGAI) of the University of La Laguna.

Synthesis of $[M_2(4,4'\text{-bpy})(Memal)_2X_2]_n$ [M = Fe(III) (2), Mn(II) (3), Co(II) (4), Ni(II) (5) and Zn(II) (6); X = Cl^-/OH^- (2) and H_2O (3–6)]. A general procedure was used for the preparation of this series of complexes. It consisted of stratifying three parts separated by water interphases (8 cm^3) in a test tube: an aqueous mixture (5 cm^3) of methylmalonic acid (0.5 mmol, 59 mg) and sodium carbonate (0.5 mmol, 53 mg) was deposited at the bottom, a solution of the divalent metal ion as its chloride salt (0.5 mmol) was placed in the middle region and 4,4′-bpy (0.5 mmol, 78 mg) dissolved in methanol (3 cm^3) on the top. The tubes were stored at room temperature, and X-ray quality crystals grew after a few weeks. The starting Fe(II) ions used in the preparation of **2** were oxidized to Fe(III) under aerobic conditions, yielding prismatic dark red single crystals. These crystals, as well as those of **3–6**, in the form of colourless (**3** and **6**), pink (**4**) or green (**5**) prisms were collected from the tube, washed with a water–ethanol mixture and air dried. Yields: *ca.* 74 (**2**), 84 (**3**), 87 (**4**), 71 (**5**) and 89% (**6**).

Anal. calc. for $C_9H_8Cl/OHFeNO_4$ (**2**): C, 37.87; H, 2.80; N, 4.90. Found: C, 37.59; H, 2.75; N, 4.81%. Anal. calc. for $C_9H_{10}MnNO_5$ (**3**): C, 40.33; H, 3.73; N, 5.22. Found: C, 40.25; H, 3.65; N, 5.18%. Anal. calc. for $C_9H_{10}CoNO_5$ (**4**): C, 39.88; H, 3.69; N, 5.17. Found: C, 38.69; H, 3.67; N, 5.13%. Anal. calc. for $C_9H_{10}NNiO_5$ (**5**): C, 39.92; H, 3.69; N, 5.17. Found: C, 39.79; H, 3.65; N, 5.11%. Anal. calc. for $C_9H_{10}NO_5Zn$ (**6**): C, 38.95; H, 3.60; N, 5.05. Found: C, 38.87; H, 3.53; N, 5.01%.

Selected IR (KBr, cm^{-1}): 3237 w, 1557 vs, 1444 m, 1336 s, 696 s, 660 s (**2**); 3245 w, 1560 vs, 1443 m, 1331 s, 689 s, 660 s (**3**); 3203 w, 1556 vs, 1445 m, 1335 m, 813 m, 704 s (**4**); 3173 w, 1558 vs, 1445 m, 1334 m, 813 s, 712 s, 665 m (**5**); 3188 w, 1560 s, 1447 m, 1331 m, 813 m, 697 vs (**6**).

$\{[Cu(4,4'\text{-bpy})_2][Cu(4,4'\text{-bpy})_2(Memal)(NO_3)(H_2O)]\}_n{\cdot}nNO_3{\cdot}3.5nH_2O$ (7). A methanolic solution (5 cm^3) of 4,4′-bpy (0.5 mmol, 78 mg) was added dropwise to an aqueous solution (10 cm^3) of copper(II)-methylmalonate (0.5 mmol, 90 mg) under continuous stirring; a pale blue solid resulted after the addition of a few drops. The filtration of this product gave a clear blue solution that was allowed to evaporate at room temperature. X-Ray quality blue plates of **7** grew after a few days (yield *ca.* 20%, based on copper). Anal. calc. for $C_{44}H_{45}Cu_2N_{10}O_{14.5}$ (**7**): C, 48.86; H, 4.20; N, 12.94; Found: C, 48.76; H, 4.20; N, 12.82%.

$[Cu(4,4'\text{-bpy})_2(Memal)(H_2O)]_n{\cdot}nH_2O$ (8). A warm aqueous solution (5 cm^3) of 4,4′-bpy (2 mmol, 312 mg) was added dropwise to a hot aqueous solution (5 cm^3) of copper(II)-methylmalonate (0.5 mmol, 90 mg). The resulting blue solution was filtered to remove any solid particles, and it was then stored at 38 °C. Single crystals of **8** as blue prisms grew from this solution after a few hours. Yield *ca.* 60%. Anal. calc. for $C_{24}H_{24}CuN_4O_6$ (**8**): C, 54.61; H, 4.55; N, 10.61; Found: C, 54.50; H, 4.47; N, 10.55%.

Physical techniques

The IR spectra (450–4000 cm^{-1}) of **2–8** as KBr pellets were recorded on a Bruker IF S66 spectrophotometer with an ATR

module for solid samples by the SEGAI service of the University of La Laguna. Magnetic susceptibility measurements on polycrystalline samples of **2–8** were performed in a Quantum Design SQUID magnetometer over the temperature range 1.9–295 K. Diamagnetic corrections of the constituent atoms were estimated from Pascal's constants[16] as -144×10^{-6} (**2**), -137×10^{-6} (**3**), -134×10^{-6} (**4** and **5**), -138×10^{-6} (**6**), -301×10^{-6} (**7**) and -304×10^{-6} cm^3 mol^{-1} (**8**) [per mol of M(III) (**2**)/M(II) (**3–8**)]. Experimental magnetic susceptibilities were also corrected for magnetization of the sample holder (**2–8**) and temperature-independent paramagnetism [60×10^{-6} cm^3 mol^{-1} per Cu(II) (**7** and **8**) and 100×10^{-6} cm^3 mol^{-1} per Ni(II) (**5**)].

Crystallographic data collection and structure determination

Single crystals of **2–8** were mounted on a Bruker Nonius KappaCCD diffractometer and crystallographic data were collected at 293(2) K using graphite-monochromated Mo-K$_\alpha$ radiation (λ = 0.71073 Å). The data collection was carried out with φ–ω scans in the 2.8–27.5° (**2**), 3.4–30° (**3**), 3.0–27.5 (**4**), 4.5–30.0° (**6**), 4.6–27.5° (**7**) and 4.04–27.50 (**8**) θ ranges. A SADABS absorption correction was applied to the collected data for these complexes.[17] The crystal structures were solved by direct methods and refined by the full-matrix least-squares technique on F^2 using the SHELXS-97 and SHEXL-97 programs[18] included in the WINGX software package.[19] All non-hydrogen atoms were refined anisotropically. The final geometrical calculations and graphical manipulations were carried out using the PARST95[20] and DIAMOND[21] programs. A summary of the crystallographic data and structure refinement of complexes **2–8** is given in Table 1. The main bond lengths and angles for **2–8** are listed in Table 2 (**2–6**) and Table 3 (**7** and **8**). The hydrogen bonds (**3–8**) are grouped in Table 4.

A single crystal of **7** is shown in Fig. 1. It appears as an octagonal prism with a subtle cross on the surface, which delimits four areas of different blue shades with opposite zones having the same colour. At first, not much attention was paid to this fact, and a well-shaped high quality crystal was mounted for X-ray measurements. The cell measurement gave a tetragonal space group with good σ-deviations; data reduction led to R_{sym} = 0.042. The structure was solved by direct methods using SHELXS-97 in the $P4_2/n$ space group, but the refinement always failed. The good experimental data (R_{sym} for triclinic space group being 0.041), the failure of the refinement and the tetragonal space group pointed out the possibility of merohedral twinning, but a few attempts to solve it were not successful. After this, we recalled the morphology of the crystal and the two different blue areas separated by a subtle cross. We carefully broke the crystal to separate the two areas, mounting both crystals for further X-ray measurements. The new space group was orthorhombic with the values of the cell parameters a, b and c being very similar to those found in the first measurement. The structure was finally solved in the orthorhombic non-centrosymmetric $Pc2_1n$ space group with a Flack parameter of 0.019(15).[22] The experimental data of the other phase (the other crystal area) was refined using the atomic positions of the first phase and led to a Flack parameter close to one, supporting the notion that two enantiomorphs were formed within the same crystal.

Results and discussion

Description of the structures. [M$_2$(4,4′-bpy)(Memal)$_2$X$_2$]$_n$ (2–6)] [M = Fe(III) (2), Mn(II) (3), Co(II) (4), Ni(II) (5) and Zn(II) (6); X = Cl$^-$/OH$^-$ (2) and H$_2$O (1 and 3–6)]

2–6 are isomorphous compounds whose structure is made up of corrugated (4,4) square grids of carboxylate(methylmalonate)-bridged M(II) [M = Mn (**3**), Co(**4**) Ni(**5**) and

Table 1 Crystallographic data for complexes **2–8**

	2	**3**	**4**	**6**	**7**	**8**
Formula	$C_9H_{8.90}FeNO_{4.90}Cl_{0.10}$	$C_9H_{10}MnNO_5$	$C_9H_{10}CoNO_5$	$C_9H_{10}ZnNO_5$	$C_{44}H_{46}O_{15}N_{10}Cu_2$	$C_{24}H_{24}O_6N_4Cu$
FW	268.87	267.12	271.11	277.55	1081.90	527.978
Crystal system	Monoclinic	Monoclinic	Monoclinic	Monoclinic	Orthorhombic	Monoclinic
Space group	$P2_1/n$	$P2_1/n$	$P2_1/n$	$P2_1/n$	$Pc2_1n$	$P2_1/n$
a/Å	7.3274(3)	7.4182(4)	7.2184(4)	7.2498(5)	15.814(2)	7.4191(3)
b/Å	19.6916(8)	19.4547(9)	19.8049(9)	19.7336(12)	15.9037(10)	27.4874(13)
c/Å	7.3642(3)	7.4673(3)	7.3177(4)	7.3271(4)	18.4974(16)	11.5347(11)
β (°)	91.750(3)	91.812(5)	91.704(4)	91.714(5)	—	91.609(6)
V/Å^3	1062.07(7)	1077.13(9)	1045.67(9)	1047.78(11)	4652.3(8)	2351.4(3)
Z	4	4	4	4	4	4
μ(Mo-K$_\alpha$)/cm^{-1}	1.448	1.230	1.646	2.349	9.95	9.77
T/K	293(2)	293(2)	293(2)	293(2)	293(2)	293(2)
ρ_{calc}/g cm^{-3}	1.681	1.647	1.722	1.759	1.529	1.480
λ/Å	0.71073	0.71073	0.71073	0.71073	0.71073	0.71073
Index ranges	$-9 \le h \le 9$ $-25 \le k \le 25$ $-9 \le l \le 9$	$-10 \le h \le 10$ $-27 \le k \le 27$ $-10 \le l \le 10$	$-8 \le h \le 9$ $-25 \le k \le 24$ $-9 \le l \le 9$	$-10 \le h \le 10$ $-24 \le k \le 27$ $-10 \le l \le 8$	$-18 \le h \le 20$ $-20 \le k \le 20$ $-15 \le l \le 24$	$-8 \le h \le 9$ $-35 \le k \le 32$ $-14 \le l \le 11$
Independent reflections (R_{int})	2435 (0.0253)	3143 (0.0223)	2393 (0.0153)	2976 (0.0269)	10222 (0.0519)	5318 (0.0495)
Flack parameter	—	—	—	—	0.019(15)	—
Observed reflections [$I > 2\sigma(I)$]	2008	2708	2223	2435	6732	3164
Parameters	186	190	190	190	669	316
Goodness-of-fit	1.118	1.090	1.114	1.062	1.054	1.058
R [$I > 2\sigma(I)$]	0.0351	0.0344	0.0225	0.0297	0.0597	0.0723
R_w [$I > 2\sigma(I)$]	0.0776	0.0810	0.0557	0.0593	0.1250	0.1522
R (all data)	0.0494	0.0434	0.0255	0.0439	0.1117	0.1345
R_w (all data)	0.0830	0.0847	0.0568	0.0633	0.1470	0.1764

Table 2 Selected bond lengths (Å) and angles (°) for **2–6**

2					
Fe(1)–O(2)	2.0986(17)	O(2)–Fe(1)–O(4)	83.94(7)	O(4)–Fe(1)–OH/Cl	92.74(7)
Fe(1)–O(1a)	2.1143(17)	O(1a)–Fe(1)–O(4)	88.00(7)	O(3b)–Fe(1)–OH/Cl	89.57(7)
Fe(1)–O(4)	2.1206(16)	O(2)–Fe(1)–O(3b)	90.09(7)	O(2)–Fe(1)–N(1)	87.63(8)
Fe(1)–O(3b)	2.1280(17)	O(1a)–Fe(1)–O(3b)	97.80(7)	O(1a)–Fe(1)–N(1)	88.92(7)
Fe(1)–OH/Cl	2.1811(18)	O(4)–Fe(1)–O(3b)	173.65(7)	O(4)–Fe(1)–N(1)	91.07(7)
Fe(1)–N(1)	2.206(2)	O(2)–Fe(1)–OH/Cl	91.27(7)	O(3b)–Fe(1)–N(1)	86.48(7)
O(2)–Fe(1)–O(1a)	171.17(7)	O(1a)–Fe(1)–OH/Cl	92.73(7)	OH/Cl–Fe(1)–N(1)	175.90(8)
3					
Mn(1)–O(2)	2.1562(14)	O(2)–Mn(1)–O(4)	82.68(5)	O(4)–Mn(1)–O(1W)	94.14(6)
Mn(1)–O(1a)	2.1618(14)	O(1a)–Mn(1)–O(4)	87.46(5)	O(3b)–Mn(1)–O(1W)	88.58(5)
Mn(1)–O(4)	2.1668(13)	O(2)–Mn(1)–O(3b)	89.37(6)	O(2)–Mn(1)–N(1)	87.34(6)
Mn(1)–O(3b)	2.1754(14)	O(1a)–Mn(1)–O(3b)	100.30(6)	O(1a)–Mn(1)–N(1)	89.36(6)
Mn(1)–O(1W)	2.2217(15)	O(4)–Mn(1)–O(3b)	171.67(6)	O(4)–Mn(1)–N(1)	91.48(6)
Mn(1)–N(1)	2.2824(16)	O(2)–Mn(1)–O(1W)	91.80(6)	O(3b)–Mn(1)–N(1)	85.64(6)
O(2)–Mn(1)–O(1a)	169.52(6)	O(1a)–Mn(1)–O(1W)	92.46(5)	O(1W)–Mn(1)–N(1)	174.16(6)
4					
Co(1)–O(1a)	2.0923(12)	O(1a)–Co(1)–O(2)	171.91(5)	O(2)–Co(1)–O(1W)	90.76(5)
Co(1)–O(4)	2.0888(11)	O(4)–Co(1)–O(2)	85.61(5)	O(3b)–Co(1)–O(1W)	90.28(5)
Co(1)–O(2)	2.0660(12)	O(1a)–Co(1)–O(3b)	97.52(5)	O(1a)–Co(1)–N(1)	87.86(5)
Co(1)–O(3b)	2.1040(12)	O(4)–Co(1)–O(3b)	174.39(5)	O(4)–Co(1)–N(1)	91.46(5)
Co(1)–O(1W)	2.1369(12)	O(2)–Co(1)–O(3b)	89.25(5)	O(2)–Co(1)–N(1)	88.18(5)
Co(1)–N(1)	2.1586(14)	O(1a)–Co(1)–O(1W)	93.62(5)	O(3b)–Co(1)–N(1)	86.15(5)
O(1a)–Co(1)–O(4)	87.44(5)	O(4)–Co(1)–O(1W)	92.01(5)	O(1W)–Co(1)–N(1)	176.29(5)
6					
Zn(1)–O(2)	2.0880(14)	O(2)–Zn(1)–O(4)	85.17(5)	O(4)–Zn(1)–O(1W)	92.18(6)
Zn(1)–O(1a)	2.1000(13)	O(1a)–Zn(1)–O(4)	87.53(5)	O(3b)–Zn(1)–O(1W)	89.72(5)
Zn(1)–O(4)	2.1013(13)	O(2)–Zn(1)–O(3b)	89.14(5)	O(2)–Zn(1)–N(1)	87.99(6)
Zn(1)–O(3b)	2.1229(13)	O(1a)–Zn(1)–O(3b)	98.00(6)	O(1a)–Zn(1)–N(1)	88.29(6)
Zn(1)–O(1W)	2.1248(15)	O(4)–Zn(1)–O(3b)	174.02(5)	O(4)–Zn(1)–N(1)	91.98(6)
Zn(1)–N(1)	2.1614(16)	O(2)–Zn(1)–O(1W)	90.61(6)	O(3b)–Zn(1)–N(1)	85.96(6)
O(2)–Zn(1)–O(1a)	171.69(5)	O(1a)–Zn(1)–O(1W)	93.64(5)	O(1W)–Zn(1)–N(1)	175.48(6)

$a = x - \frac{1}{2}, -y + \frac{1}{2}, z - \frac{1}{2}$; $b = x - \frac{1}{2}, -y + \frac{1}{2}, z + \frac{1}{2}$.

Table 3 Selected bond lengths (Å) and angles (°) for **7** and **8**

7			
Cu(1)–O(2)	1.908(3)	Cu(2)–N(5)	2.080(4)
Cu(1)–O(4)	1.936(3)	Cu(2)–N(6c)	2.081(4)
Cu(1)–N(1)	2.042(4)	Cu(2)–N(7)	2.060(4)
Cu(1)–N(3)	2.002(4)	Cu(2)–N(8d)	2.079(4)
Cu(1)–O(1W)	2.394(5)	Cu(2)–O(1e)	2.397(3)
Cu(1)–O(5)	2.692(6)	Cu(2)–O(3)	2.331(3)
O(2)–Cu(1)–O(4)	92.31(12)	N(5)–Cu(2)–N(6c)	178.11(18)
O(2)–Cu(1)–N(1)	87.68(14)	N(5)–Cu(2)–N(7)	88.82(17)
O(2)–Cu(1)–N(3)	173.08(19)	N(5)–Cu(2)–N(8d)	90.97(16)
O(2)–Cu(1)–O(1W)	92.93(18)	N(5)–Cu(2)–O(1e)	94.93(15)
O(2)–Cu(1)–O(5)	86.8(2)	N(5)–Cu(2)–O(3)	88.56(16)
O(4)–Cu(1)–N(1)	173.92(19)	N(6c)–Cu(2)–N(7)	91.52(16)
O(4)–Cu(1)–N(3)	87.33(14)	N(6c)–Cu(2)–N(8d)	88.61(16)
O(4)–Cu(1)–O(1W)	84.30(18)	N(6c)–Cu(2)–O(1e)	83.22(14)
O(4)–Cu(1)–O(5)	103.4(2)	N(6c)–Cu(2)–O(3)	93.26(14)
N(1)–Cu(1)–N(3)	93.41(15)	N(7)–Cu(2)–N(8d)	177.42(18)
N(1)–Cu(1)–O(1W)	89.63(18)	N(7)–Cu(2)–O(1e)	88.32(15)
N(1)–Cu(1)–O(5)	82.7(2)	N(7)–Cu(2)–O(3)	94.87(15)
N(3)–Cu(1)–O(1W)	93.90(18)	N(8d)–Cu(2)–O(1e)	89.14(15)
N(3)–Cu(1)–O(5)	86.8(2)	N(8d)–Cu(2)–O(3)	87.69(15)
O(1W)–Cu(1)–O(5)	172.2(2)	O(1e)–Cu(2)–O(3)	175.32(14)
8			
Cu(1)–O(1)	1.943(3)	O(1)–Cu(1)–O(1W)	79.06(15)
Cu(1)–O(4f)	1.930(3)	O(4f)–Cu(1)–N(1)	88.66(14)
Cu(1)–N(1)	2.064(4)	O(4f)–Cu(1)–N(3)	90.54(15)
Cu(1)–N(3)	2.050(4)	O(4f)–Cu(1)–O(1W)	114.85(16)
Cu(1)–O(1W)	2.289(4)	N(1)–Cu(1)–N(3)	173.62(16)
O(1)–Cu(1)–O(4f)	165.94(15)	N(1)–Cu(1)–O(1W)	91.66(1)
O(1)–Cu(1)–N(1)	88.86(14)	N(3)–Cu(1)–O(1W)	94.42(15)
O(1)–Cu(1)–N(3)	90.39(15)		

$c = -x + 1, y + \frac{1}{2}, -z + 1$; $d = -x + 2, y + \frac{1}{2}, -z + 1$; $e = -x + \frac{3}{2}, y, z + \frac{1}{2}$; $f = x + \frac{1}{2}, -y + \frac{1}{2}, z + \frac{1}{2}$.

Table 4 Hydrogen bond distances (Å) and angles (°) for complexes **3**, **4**, **6–8**

3				
D–H···A[a]	D–H	H···A	D···A	D–H···A
O(1W)–H(1WA)···O(2a)	0.80(3)	1.96(3)	2.719(2)	157(3)
O(1W)–H(1WB)···O(4b)	0.91(3)	1.87(3)	2.748(2)	162(3)
4				
D–H···A[a]	D–H	H···A	D···A	D–H···A
O(1W)–H(1WA)···O(2a)	0.88(2)	1.82(3)	2.665(3)	161(3)
O(1W)–H(1WB)···O(4b)	0.79(2)	1.96(3)	2.714(3)	160(3)
6				
D–H···A[a]	D–H	H···A	D···A	D–H···A
O(1W)–H(1WA)···O(2a)	0.86(3)	1.84(2)	2.664(3)	161(2)
O(1W)–H(1WB)···O(4b)	0.77(3)	1.97(2)	2.705(3)	162(2)
7				
D–H···A[a]	D–H	H···A	D···A	D–H···A
N(2)···O(4W)	—	—	2.87(1)	—
N(4)···O(3W)	—	—	2.84(1)	—
O(8)···O(4W)	—	—	3.03(2)	—
O(1W)···O(2W)	—	—	2.796(10)	—
O(1W)···O(4W)	—	—	2.721(12)	—
O(1W)···O(4)	—	—	2.927(7)	—
O(2W)···O(3W)	—	—	2.666(11)	—
O(2W)···O(10)	—	—	2.682(17)	—
O(3W)···O(7)	—	—	2.734(16)	—
O(4W)···O(8)	—	—	3.01(2)	—
O(5W)···O(7)	—	—	2.87(3)	—
8				
O(1w)–H···O(2h)	—	—	2.725(5)	—
O(1w)–H···O(2wh)	—	—	2.905(7)	—
O(2w)–H···O(4)	—	—	2.916(6)	—
O(2w)–H···O(3j)	—	—	2.967(7)	—

$a = x - \frac{1}{2}, -y + \frac{1}{2}, z - \frac{1}{2}$; $b = x + \frac{1}{2}, -y + \frac{1}{2}, z - \frac{1}{2}$; $h = x + 1, y, z$; $j = x - 1, y, z$.

[a] D and A stand for donor and acceptor, respectively.

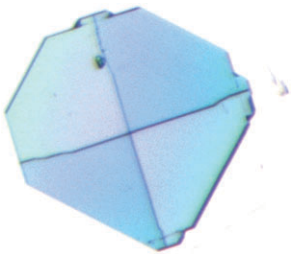

Fig. 1 Microscope image of a 'single' crystal of complex **7**. Four regions are observed with a subtle colour difference between them.

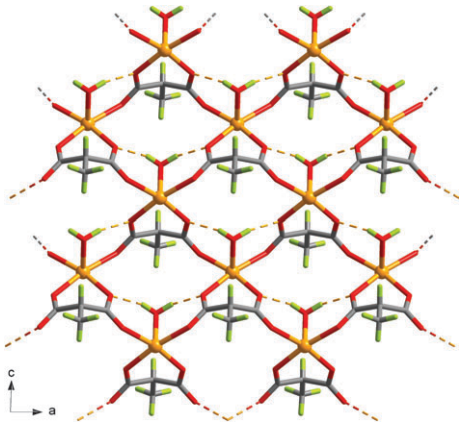

Fig. 2 Perspective views of a fragment of the carboxylate(methylmalonate)-bridged square grid of the metal ions in **1–6** extending in the *ac* plane. The 4,4′-bpy ligand has been removed for clarity.

Zn (**6**)] or M(III) [M = Fe (**2**)] that grow in the *ac* plane (Fig. 2) and which are pillared through bis-monodentate 4,4′-bpy along the *b* axis to afford a three-dimensional network (Fig. 3 and Fig. 4). This structure is the same as that previously reported for **1**. The crystallographically independent units of **2** and **3–6** are shown in Fig. 5. The layers in **1–6** are analogous to that previously reported in $[Cu(Memal)(H_2O)]_n$[15a] and they are also similar to those occurring in the Cu(II)-Phmal,[14e] Cu(II)-cyclobutanemalonate[23] and Mn(II)-mal complexes.[6c] Considering the carboxylate bridge as the unique connector within the *ac* plane, the 3D structure can be topologically described as a $[4^4 6^6]$-**sqp** net in the Schläfli notation.[24] The size of the methyl group of the methylmalonate ligand is small enough to allow the 4,4′-bpy ligand to connect the layers in **1–6**, in contrast to what occurs in the related system with a phenylmalonate ligand. The 4,4′-bpy molecule is located alternatively above and below each layer, practically in a *trans* position with respect to the methyl group of the Memal ligand. The shortest centroid–centroid distances between adjacent pyridyl rings vary in the range 7.239(4) (**1**) to 7.467(3) Å (**3**), values which rule out any π-type interaction in this family of compounds.[25] Weak CH/π interactions with the methyl groups pointing toward the aromatic rings are observed in the structures, with CH/centroid distances covering the range 4.192(2) (**3**) to 4.461(2) Å (**4**). In fact, these values are in the upper limit for this kind of interaction.[26] Intralayer hydrogen bonds involving the coordinated water molecule and oxygen atoms of the methylmalonate ligand in **1** and **3–6** contribute to the stabilization of the structure [see Table 4].

The metal ions in **2–6** are six-coordinated with MNO_4OH/Cl (**2**) and MNO_4O_W (**3–6**) chromophores in distorted octahedral environments formed by four methylmalonate oxygens, one 4,4′-bpy nitrogen atom (**2–6**) and a chloro/hydroxo (**2**) or a water molecule (**3–6**), the degree of distortion depending on the metal ion involved. In fact, the octahedron in **2–6** is slightly elongated with the parameters *s*/*h* and ϕ being 1.247 and 58.71° for OH and 1.267 and 58.01° for Cl (**2**), 1.252 and 58.50° (**3**), 1.280 and 62.57° (**4**), and 1.237 and 59.20° (**6**) [values for an ideal octahedron are 1.22 and 60° for s/h and ϕ, respectively].[27] Four methylmalonate oxygen atoms [O(1), O(2), O(3) and O(4); average M–O bond distance being

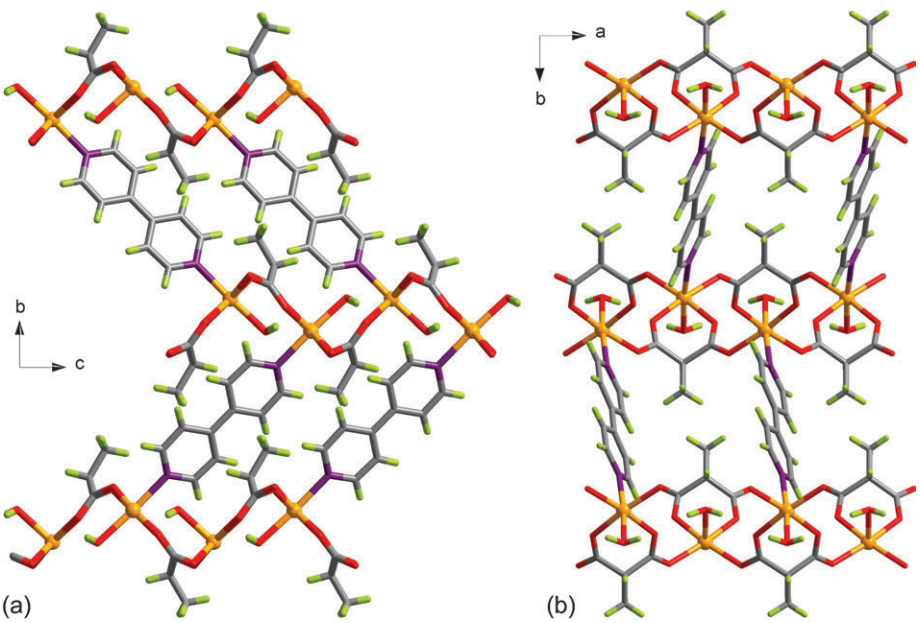

Fig. 3 Perspective views of the crystal packing of **1** and **3–6** along the *a* (a) and *c* (b) axes.

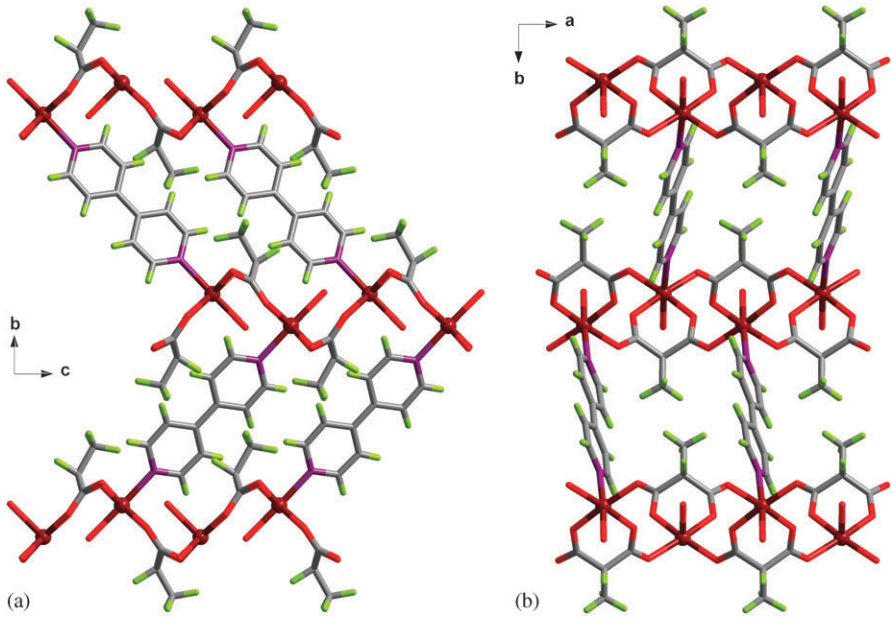

Fig. 4 Perspective views of the crystal packing of **2** along the *a* (a) and *c* (b) axes.

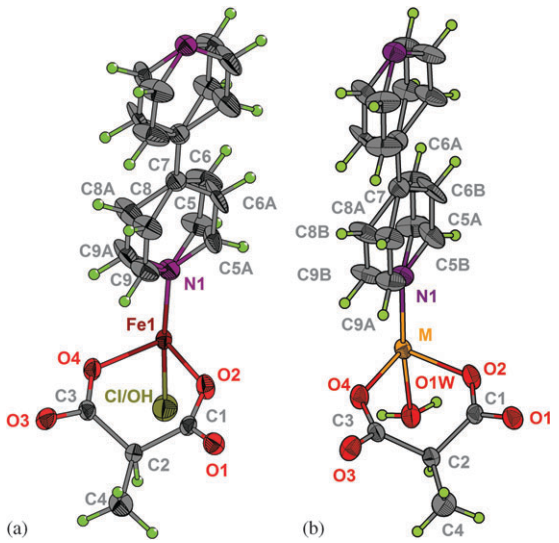

Fig. 5 Views of the crystallographically independent units of **2** (a) and **3–6** (b) [M = Mn (**3**), Co (**4**) and Zn (**6**)] showing the atom numbering. The ellipsoids are at 50% probability.

2.115(2) (**2**), 2.1650(14) (**3**), 2.0880(12) (**4**) and 2.103(2) (**6**) Å, respectively; see Table 2] build the basal plane, whereas a nitrogen atom [N(1)] from a 4,4′-bpy ligand (**2–6**) and a chloro/hydroxo (**2**) or a water molecule [O(1W)] (**3–6**) occupy the axial positions. The M–N(1) and M–O(1W) bond distances vary in the ranges 2.1585(14)–2.2824(16) and 2.1245(15)–2.2213(15) Å, respectively. In the case of related compound **1**, the octahedron around the copper(II) ion is unusually compressed, with two short bonds [1.980(4) and 2.025(4) Å for Cu(1)–O(1w) and Cu(1)–N(1), respectively] and four somewhat longer bond lengths corresponding to the oxygen atoms of the Memal ligand [values in the range 2.080(4)–2.234(5) Å]. This situation resembles that observed in the complex [Cu(2,4′-bpy)(Phmal)(H_2O)], where a deep analysis of the vibrational amplitudes describes this compression as a static pseudo-Jahn–Teller disorder.[14c]

The methylmalonate ligand in all compounds adopts simultaneously the bidentate [through O(2) and O(4), the values of the angle subtended at the metal ion being 86.64(17) (**1**), 83.94(7) (**2**), 82.68(5) (**3**), 85.61(5) (**4**) and 85.17(5)° (**6**)] and bis-monodentate [through O(1) and O(3)] coordination modes. The pyridyl rings of the 4,4′-bpy ligand in **1–6** are coplanar because they are symmetry-related with an inversion centre located at the middle of the central C–C bond between the pyridyl rings. The 4,4′-bpy group is disordered between two positions in the iron(III) (**2**), manganese(II) (**3**), cobalt(II) (**4**) and zinc(II) (**6**) complexes, with occupancy factors of 0.30 and 0.70 (**2**), 0.34 and 0.66 (**3**), 0.27 and 0.73 (**4**), and 0.28 and 0.72 (**6**), and an angle of 29.3(9) (**2**), 25.7(9) (**3**), 40.4(5) (**4**) and 38.1(5)° (**6**) between the aromatic rings.

The values of the metal–metal separations through the two crystallographically independent *anti–syn* carboxylate bridges are 5.2879(8) and 5.4482(8) (**1**), 5.4760(6) and 5.3234(6) (**2**), 5.5411(4) and 5.3808(4) (**3**), 5.4199(4) and 5.2730(4) (**4**), and 5.439(4) and 5.291(4) Å (**6**) through O(1)–C(1)–O(2) and O(3)–C(3)–O(4), respectively. The carboxylate bridges link two equatorial positions at the metal centres, the angle between adjacent equatorial planes being 89.60(7) (**1**), 88.40(5) (**2**), 88.94(3) (**3**), 87.74(2) (**4**) and 88.58(3)° (**6**). The 4,4′-bpy bridge connects two metal atoms from adjacent layers with values for the metal–metal separation in the range 11.1261(11) (**1**)–11.6535(5) Å (**3**). They are in agreement with the reported values for the metal–metal distances across 4,4′-bpy in previous structural reports.[28]

The shortest interlayer $M^{II}\cdots M^{II}$ distances [values covering the range 8.2709(10) (**1**)–8.4764(5) Å (**4**)] are shorter than those through the bridging 4,4′-bpy because of the corrugation of the layers and the non-parallel alignment of the 4,4′-bpy groups along the stacking direction, the minimum and

maximum values of the angle between the 4,4′-bpy ligand and the normal of the layer being 40.87(8) (**1**) and 45.11(7)° (**6**).

{[Cu(4,4′-bpy)$_2$][Cu(4,4′-bpy)$_2$(Memal)(NO$_3$)(H$_2$O)]}$_n$·*n*NO$_3$·3.5*n*H$_2$O (7). The structure of **7** contains square grids of $[Cu(4,4'\text{-bpy})_2]^{2n+}{}_n$ motifs growing in the *ab* plane that are pillared along the *c* axis by carboxylate–methylmalonate bridges from [Cu(4,4′-bpy)$_2$(Memal)(NO$_3$)(H$_2$O)] units to form a [4^{12}6^3]-**pcu** 3D net (Figs. 6–8).[24] The copper(II) atom [Cu(2)] of these last units is chelated by a methylmalonate group, which acts as a bis(monodentate) ligand towards the copper(II) atoms [Cu(1)] of two adjacent $[Cu(4,4'\text{-bpy})_2]^{2n+}{}_n$ square grids, thus pillaring them (Fig. 8). The (4,4) $[Cu(4,4'\text{-bpy})_2]^{2n+}{}_n$ grid provides channels of dimensions 11 × 11 Å^2 along the *c* axis, which are filled by the terminal 4,4′-bpy molecules of the pillaring units, nitrate anions and water of crystallization molecules (Fig. 7b). An intricate network of hydrogen bonds among the water and nitrate groups contributes to the stabilization of the structure [O···O distances in the range 2.56(3)–2.728(15) Å]. The terminal 4,4′-bpy ligands establish hydrogen bonds with the water of crystallization molecules [2.869(12) and 2.845(10) Å for N(2)···O(5WC) and N(4)···O(3w), respectively] (Table 4). They are also involved in weak π-type interactions among them, and with the $[Cu(4,4'\text{-bpy})_2]^{2+}{}_n$ 2D network, fixing their position in the channels. The values of the centroid–centroid distances between the pyridyl rings covers the range 3.779(8)–3.942(7) Å, and those of the offset angle (defined between the centroid–centroid vector and the normal to the plane of the aromatic ring) vary between 15.5(4) and 27.3(4)°. Furthermore, the terminal 4,4′-bpy groups establish weak CH/π type interactions with those of the (4,4) grid, with the C···π distances and C–H···π angles varying in the ranges 3.444(7)–4.011(6) Å and 144.5(4)–165.9(4)°, respectively.

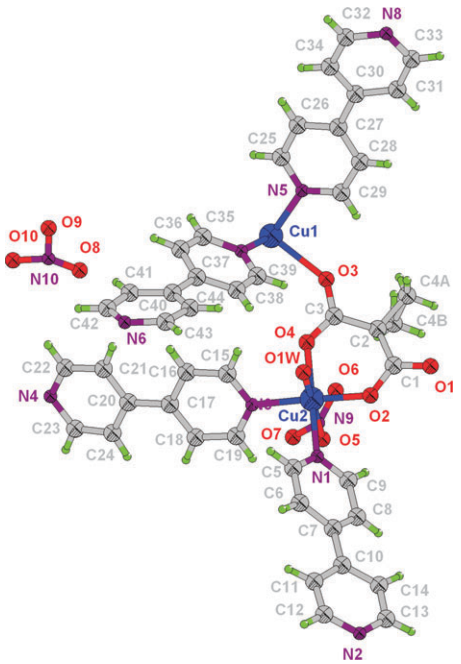

Fig. 6 A view of the asymmetric unit of **7** along with the numbering scheme.

Two crystallographically independent copper(II) ions [Cu(1) and Cu(2)] occur in **7** (Fig. 6). They exhibit a distorted octahedral environment, the values of the parameters *s*/*h* and ϕ being 1.31 and 56.2° [Cu(1)], and 1.45 and 54.4° [Cu(2)].[27] Four 4,4′-bpy nitrogen atoms [N(5), N(6), N(7) and N(8) with an average Cu–N bond distance of 2.075(4) Å] build the equatorial plane at Cu(1), whereas two malonate oxygen atoms fill the axial positions [O(1) and O(3); mean Cu(1)–O bond distance = 2.364(3) Å]. Two nitrogen atoms of the 4,4′-bpy ligands [N(1) and N(3); average Cu(2)–N bond distance of 2.021(4) Å] and two methylmalonate oxygen atoms [O(2) and O(4); average Cu(2)–O bond distance of 1.922(3) Å] build the basal plane at Cu(2), while the axial positions are occupied by a water molecule [Cu(2)–O(1W) = 2.395(5) Å] and a nitrate-oxygen atom [Cu(2)–O(5) = 2.692(6) Å].

The methylmalonate ligand adopts simultaneously bidentate [through O(2) and O(4) toward Cu(2), the angle subtended at the copper atom being 92.30(12)°] and bis-monodentate [through O(3) and O(1) toward Cu(1) and Cu(1g), respectively; $g = -x + \frac{3}{2}, y, z - \frac{1}{2}$] coordination modes, the Cu(1)···Cu(1g) separation being 9.2487(1) Å. The four crystallographically independent 4,4′-bpy ligands present in **7** exhibit two different coordination modes: two of them act as monodentate ligands toward Cu(2), constituting the terminal groups of the pillaring unit, while the other two act as bis-monodentate ligands toward Cu(1), being responsible for the construction of the square grid. The pyridyl rings of the 4,4′-bpy ligands are planar, but the whole molecules are not [the values of the dihedral angle between the pyridyl rings vary in the range 8.2(1)–25.3(2)°], the deviation from the planarity being smaller for the terminal 4,4′-bpy groups.

The copper–copper separation through the bridging 4,4′-bpy ligand within the square grid of $[Cu(4,4'\text{-bpy})_2]^{2n+}{}_n$ is 11.2198(12) Å, whereas the Cu(1)···Cu(2) separation across the two crystallographically independent carboxylate-methylmalonate bridges O(3)–C(3)–O(4) and O(1)–C(1)–O(2) are 5.6430(9) and 5.6248(9) Å, respectively. Both carboxylate bridges exhibit the *anti–syn* conformation and they link one axial position at Cu(1) with an equatorial one at Cu(2).

The structure of **7** resembles that of the family of compounds of formula $[Cu(A)_x(4,4'\text{-bpy})_2]_n \cdot mH_2O$ [A is an anion such as $[SiF_6]^{2-}$ or $[GeF_6]^{2-}$ ($x = 1$), or $[PF_6]^-$ ($x = 2$)] that were reported by Kitagawa's group.[29] The structure of $[Cu(SiF_6)(4,4'\text{-bpy})_2]_n \cdot 8nH_2O$ consists of a 3D-network based on a square grid of $[Cu(4,4'\text{-bpy})_2]^{2n+}{}_n$ that is pillared by SiF_6^{2-} anions, as in **7**, but the pillars in this compound are the $[Cu(4,4'\text{-bpy})_2(Memal)(NO_3)(H_2O)]^-$ units. Other than this, the main differences between their structures are the cationic character of the 3D-network of **7** and the presence of the terminal 4,4′-bpy ligands in the channels, where only crystallization water molecules can be found in Kitagawa's complex. The existence of a coordination polymer such as **7** shows the robustness of the 2D $[Cu(4,4'\text{-bpy})_2]^{2n+}{}_n$ network, which can be pillared through bulkier groups than $[EF_6]^{p-}$ [E = Si and Ge ($p = 2$) and P ($p = 1$)] anions.

[Cu(4,4′-bpy)$_2$(Memal)(H$_2$O)]$_n$·*n*H$_2$O (8). The structure of **8** consists of chains of *trans*-bis(4,4′-bpy)aquacopper(II) motifs growing along the [101] direction, the bridging unit being the

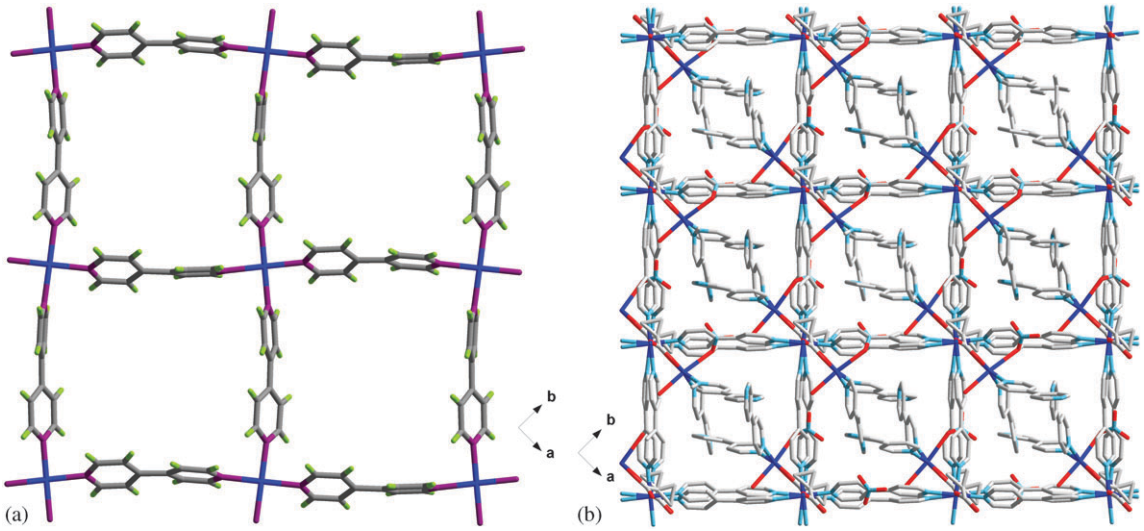

Fig. 7 Perspective views along the *c* axis of the structure of **7** showing (a) the (4,4) $[Cu(4,4'\text{-bpy})_2]^{2n+}{}_n$ square grid and (b) the crystal packing.

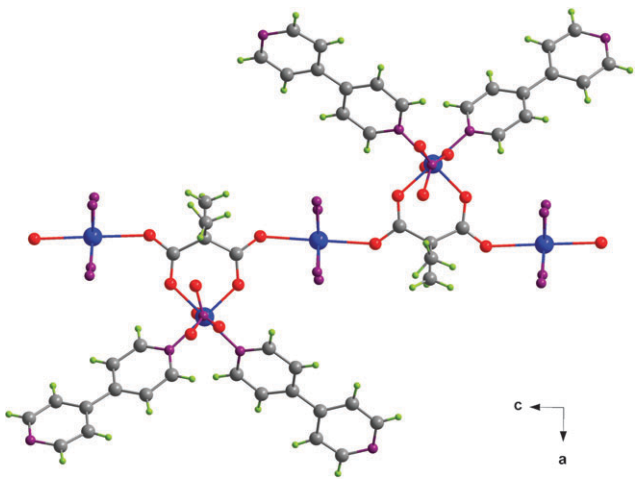

Fig. 8 A view down the *c* axis showing the pillaring units that connect the parallel $[Cu(4,4'\text{-bpy})_2]^{2n+}{}_n$ grids in the crystal structure of **7** (the bridging 4,4′-bpy ligands are omitted for clarity).

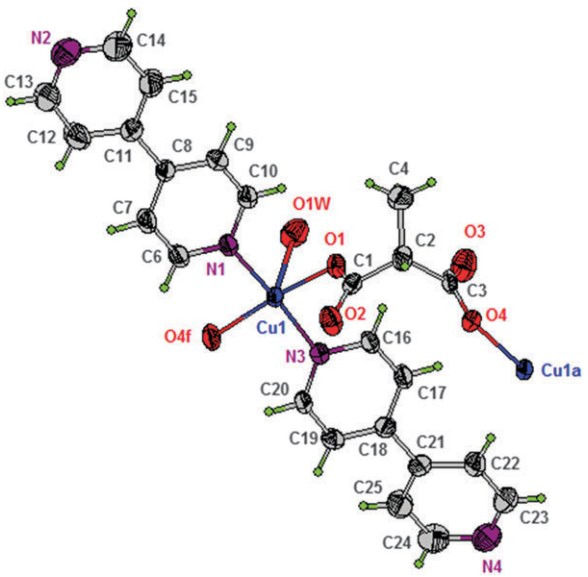

Fig. 9 A view of the asymmetric unit of **8** with the numbering scheme [a = $x - \frac{1}{2}, -y + \frac{1}{2}, z - \frac{1}{2}$; f = $x + \frac{1}{2}, -y + \frac{1}{2}, z + \frac{1}{2}$]. Ellipsoids are at 50% probability.

bis-monodentate methylmalonate ligand (Figs. 9 and 10). These chains are interlinked through hydrogen bonds involving the coordinated and crystallization water molecules and the free methylmalonate oxygen atoms [O···O distances covering the range 2.725(5)–2.967(7) Å] (see Table 4) to afford layers in the *ac* plane. These layers are further connected through π–π stacking interactions between the 4,4′-bpy ligands [the shortest centroid–centroid contact is 3.858(2) Å and the offset angle is 14.63(12)°, in agreement with previously observed pyridyl–pyridyl contacts][25] and C–H···N contacts to form a supramolecular three-dimensional network [the values of the shortest centroid–centroid separation and offset angle are 4.2428(2) Å and 33.5(2)°, respectively; D···A distances and D–H···A angles for the C(19)–H···N(2) and C(15)–H···N(4) interactions are 3.417(7) Å and 163.9(3)°, and 3.624(9) Å and 167.1(4)°, respectively].

Each copper atom in **8** exhibits a somewhat distorted square pyramidal environment, the τ value being 0.13 (τ = 0 or 1 for ideal square pyramidal or trigonal bipyramidal, respectively).[30]

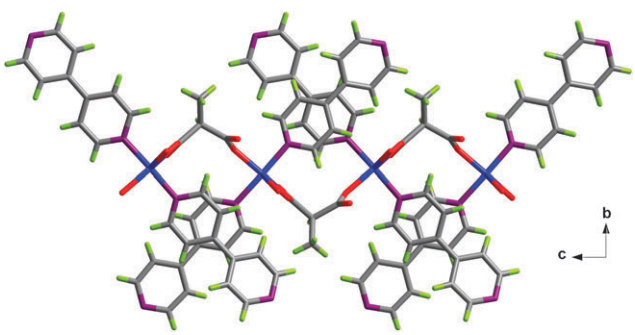

Fig. 10 A view down the *a* axis of a fragment of the malonate-bridged copper(II) chains in **8**.

Two oxygen atoms from two different methylmalonate ligands [O(1) and O(4f); the mean Cu–O(eq) bond distance being

equal to 1.936(3) Å; f = $x + \frac{1}{2}, -y + \frac{1}{2}, z + \frac{1}{2}$] and two 4,4′-bpy nitrogen atoms [N(1) and N(3); the average Cu–N bond distance is 2.057(4) Å; see Table 3] build the basal plane, while a water molecule occupies the apical position [Cu(1)–O(1w) = 2.289(4) Å]. The copper atom is shifted from the mean basal plane by 0.1866(7) Å towards the apical position.

The methylmalonate ligand exhibits an unusual *trans*-bis-monodentate coordination mode [through O(1) and O(4) to Cu(1) and Cu(1a), respectively; a = $x - \frac{1}{2}, -y + \frac{1}{2}, z - \frac{1}{2}$]. As far as we know, this coordination mode has never been observed in copper(II) complexes with Rmal ligands, but it occurs in two previous examples of malonate-containing zinc(II) compounds.[31] The two crystallographically independent 4,4′-bpy molecules act as terminally bound ligands [through N(1) and N(3) at Cu(1)] in *trans*-positions in the copper environment. The pyridyl rings of the 4,4′-bpy molecules are planar, but the whole ligands exhibit significant deviations from planarity [the values of the dihedral angles between the pyridyl rings are 27.41(18) and 12.4(2)°]. The intrachain copper–copper separation [6.7757(10) Å for Cu(1)···Cu(1b)] is somewhat shorter than the shortest interchain metal–metal distance [6.9508(10) Å for Cu(1)···Cu(1k); k = $x - \frac{1}{2}, -y + \frac{1}{2}, z + \frac{1}{2}$].

Although compounds **1–8** were prepared by reaction of the corresponding divalent metal ion with the same ligands (Memal and 4,4′-bpy), different crystal structures resulted. The Memal : 4,4′-bpy molar ratio in them [2 : 1 (**1–6**), 1 : 4 (**7**) and 1 : 2 (**8**)] accounts for this difference. The crystal structure seems to be regulated by the methylmalonate ligand in **1–6**, where square grids of carboxylate-bridged copper(II) ions are formed, as in the previously reported complex [Cu(Memal)(H_2O)].[15a] However, the structure of **7** is governed by the 4,4′-bpy ligand, which leads to the formation of the $[Cu(4,4'\text{-bpy})_2]^{2n+}{}_n$ square grid. Here, the functionality of the Cu(Memal) unit is reduced to be just a pillaring motif. Finally, the structure of **8** can be seen as an intermediate case, with the Memal ligand as a linker of the $[Cu(4,4'bpy)_2(H_2O)]^{2+}$ units but, in any case, quite different from the other Memal-containing complexes.

Magnetic properties of 2–8

The $\chi_M T$ *vs.* *T* plots for **2** and **3** [χ_M is the magnetic susceptibility per single iron(III) (**2**)/manganese(II) (**3**) ion] are practically identical (Fig. 11). At room temperature, the value of $\chi_M T$ for **2** and **3** is *ca.* 4.30 (4.47 for **2** and 4.33 for **3**) cm^3 mol^{-1} K. These are as expected for a magnetically isolated spin sextet [$\chi_M T$ = 4.375 cm^3 mol^{-1} K for S_{Fe} (**2**) = S_{Mn} (**3**) = $\frac{5}{2}$ with *g* = 2.0]. Upon cooling, $\chi_M T$ remains practically constant until 60 K, and it further decreases to reach minimum values of 0.99 (**2**) and 1.04 (**3**) cm^3 mol^{-1} K. This behaviour is indicative of the occurrence of an overall weak antiferromagnetic interaction. Although carboxylate–methylmalonate and 4,4′-bpy bridges are involved in **2** and **3**, the exchange pathway associated with the more extended 4,4-bpy ligand (metal–metal separation larger than 11 Å) can be discarded against that through the much shorter carboxylate ligand (metal–metal distance of *ca.* 5.4 Å). This simplification

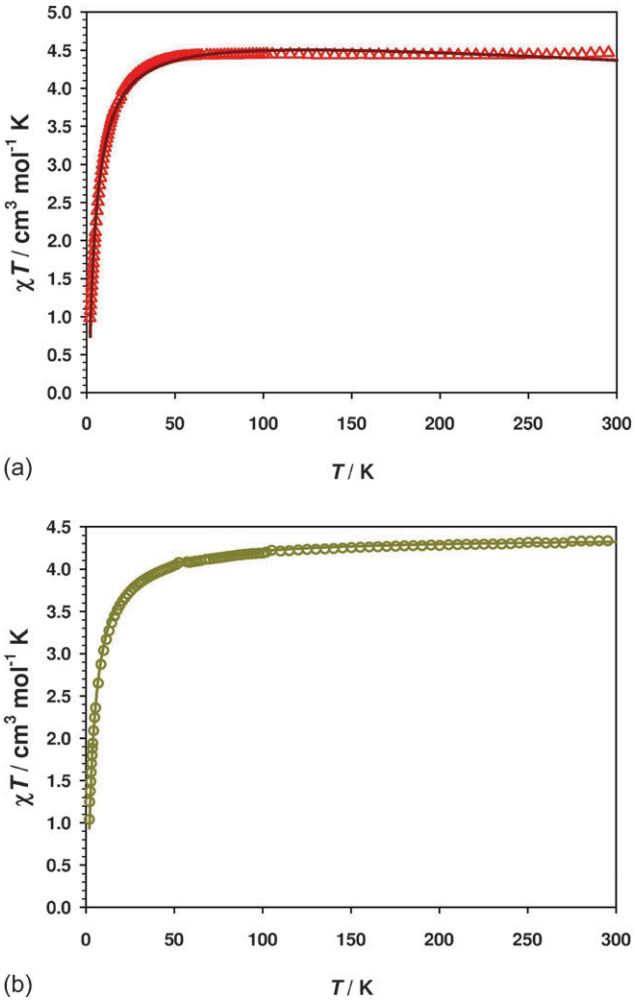

Fig. 11 $\chi_M T$ *vs.* *T* plot for **2** (△) (a) and **3** (○) (b) under applied fields of 1 T (*T* > 25 K), 0.25 T (25 K > *T* > 15 K) and 0.1 T (*T* < 15 K): the symbols represent the experimental data and the lines the best fit curve through eqn (1) (see text).

allows us to treat the magnetic data of these compounds through the Lines approach for a quadratic layer of local spin sextets that interact through *anti–syn* carboxylate bridges [eqn (1)][32a]

$$\chi_M = \frac{N\beta^2 g^2}{|J|}\left[3\Theta + \sum_{n=1}^{6}\frac{C_n}{\Theta^{n-1}}\right]^{-1} \qquad (1)$$

where $\Theta = kT/[|J|S(S+1)]$, $C_1 = 4$, $C_2 = 1.448$, $C_3 = 0.228$, $C_4 = 0.262$, $C_5 = 0.119$ and $C_6 = 0.017$, the Hamiltonian being defined as $\hat{H} = -J\sum_i \hat{S}_i \cdot \hat{S}_{i+1}$. The best least-squares fit parameters are $J = -0.269(3)$ cm^{-1}, $g = 2.00(3)$ and $R = 4.1 \times 10^{-4}$ for **2**, and $J = -0.225(2)$ cm^{-1}, $g = 2.00(1)$ and $R = 2.7 \times 10^{-4}$ for **3** (*R* is the agreement factor defined as $\Sigma_i[(\chi_M T)_{obs}(i) - (\chi_M T)_{calc}(i)]^2/\Sigma_i[(\chi_M T)_{obs}(i)]^2$). The calculated curves reproduce well the experimental data over the whole temperature range explored.

The magnetic properties of **4** in the form of a $\chi_M T$ *vs.* *T* plot [χ_M being the magnetic susceptibility per cobalt(II) ion] are shown in Fig. 12. The $\chi_M T$ at room temperature is 3.35 cm^3 mol^{-1} K [μ_{eff} per Co(II) = 5.18 $N_a\beta$ to be compared

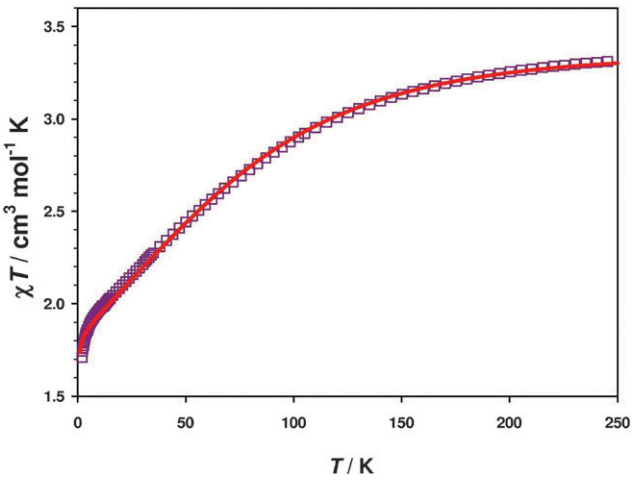

Fig. 12 A $\chi_M T$ *vs.* T plot (□) for **4** under applied fields of 1 T ($T > 25$ K), 0.1 T (25 K > $T > 15$ K) and 0.01 T ($T < 15$ K). The solid line is the best-fit curve through eqn (3) (see text).

with the spin-only value, $\mu_{eff} = 3.87\ N_a\beta$ ($g = 2.0$)], a value that is as expected for systems containing six-coordinated high-spin cobalt(II) ions with unquenched angular momentum. $\chi_M T$ decreases upon cooling to attain a value of 1.71 $cm^3\ mol^{-1}$ K at 2.0 K. This value is close to what is expected for an isolated Co^{II} ion ($\chi_M T \approx 1.75\ cm^3\ mol^{-1}$ K).[33] No maximum of the magnetic susceptibility in the $\chi_M T$ *vs.* T plot is observed in the temperature range studied. The decrease of $\chi_M T$ could be due to antiferromagnetic interactions between the cobalt(II) ions and/or depopulation of the higher energy Kramers doublets of the cobalt(II) centres. In a first approach, we will try to reproduce the magnetic behaviour of **4** by considering the Co(II) ions magnetically isolated through the Hamiltonian [eqn (2)]

$$\hat{H} = \alpha\lambda\hat{L}\hat{S} + \Delta(\hat{L}_z^2 - \tfrac{2}{3}) + \beta H(-\alpha\hat{L} + g_e\hat{S}) \qquad (2)$$

The first term accounts for the spin–orbit coupling effects, defined as $\alpha = A\kappa$; with A being a parameter whose value depends on the strength of the crystal field [its value varies between $\frac{3}{2}$ (weak crystal field) and 1 (strong crystal field)],[34] and κ being the orbital reduction factor. The inclusion of the A factor is due to the use of T–P isomorphism.[35] The second term of the Hamiltonian is the one-center operator that is responsible for the axial distortion of the six-coordinated Co(II) ion, Δ being the energy gap between the singlet $^4A_2$ and doublet ^4E levels issued from the splitting of the orbital triplet $^4T_{1g}$ ground state under axial distortion. The last term is the Zeeman interaction. The best-fit parameters through this assumption by using matrix diagonalization techniques are $\alpha = -0.38$, $\Delta = -594\ cm^{-1}$ and $\lambda = -134\ cm^{-1}$. The calculated curve matches well with the experimental data in the high-temperature domain, $15 < T < 250$ K. At very low temperatures, the magnetic data are below the calculated curve, indicating the occurrence of weak antiferromagnetic coupling. On the basis of previous magneto-structural studies, it has been shown that weak interactions can be mediated by *anti-syn* carboxylate bridges,[36] whereas they are negligible across bridging 4,4′-bpy.[37] We analyzed the magnetic data of **4** by means of expression of the magnetic susceptibility of a square layer of interacting spin doublets proposed by Lines [(eqn (3)].[32]

$$\chi_M = \frac{9N\beta^2}{25|J|} g_0^2 \left[3\Theta + \sum_{n=1}^{6} \frac{C_n}{\Theta^{n-1}}\right]^{-1} \qquad (3)$$

with $\Theta = 12kT/25|J|$, $C_1 = 4$, $C_2 = 2.667$, $C_3 = 1.185$, $C_4 = 0.149$, $C_5 = -0.191$ and $C_6 = 0.001$. However, this approach is only valid for six-coordinated Co(II) ions where the ground spin doublet is the only populated level ($T < 30$ K).[16] To expand this treatment to the whole temperature range, some of us have developed a strategy that consists of the replacement of the value of g_0 by the $G(T,J)$ function.[38] This function takes into account the λ, α and Δ parameters defined in eqn (2). The analysis of the magnetic data of **4** through the eqn (3), where g_0 is replaced by the $G(T,J)$ function, leads to the following best-fit parameters: $J = -0.05\ cm^{-1}$, $\alpha = 1.39$, $\Delta = -560\ cm^{-1}$, $\lambda = -125\ cm^{-1}$ and $R = 2.3 \times 10^{-5}$. The calculated curve reproduces very well the experimental data across the whole temperature range. The magnetic coupling between the Co(II) ions through the *anti–syn* carboxylato bridge is very weak, in agreement with previous studies,[36] and the values of α, Δ and λ are within the range of those observed in other six-coordinate high-spin cobalt(II) complexes.[33,36,37]

The magnetic behaviour of **5** in the form of a $\chi_M T$ *vs.* T plot [χ_M being the magnetic susceptibility per nickel(II) ion] is shown in Fig. 13. At room temperature, $\chi_M T$ is equal to 1.22 $cm^3\ mol^{-1}$ K, a value that is as expected for a magnetically isolated spin triplet ($\chi_M T = 1.21\ cm^3\ mol^{-1}$ K with $g = 2.20$). Upon cooling, $\chi_M T$ smoothly increases to reach a value of 1.96 $cm^3\ mol^{-1}$ K at 2.0 K. This behaviour is indicative of an overall ferromagnetic coupling. The magnetization *vs.* H plot at 2.0 K supports the occurrence of a ferromagnetic interaction (see the inset of Fig. 13), the value of the magnetization at 5 T (the maximum field available in our magnetometer) being 1.93 $N_a\beta$. This value is somewhat below that expected for a spin triplet (*ca.* 2.20 $N_a\beta$ with $g = 2.20$),

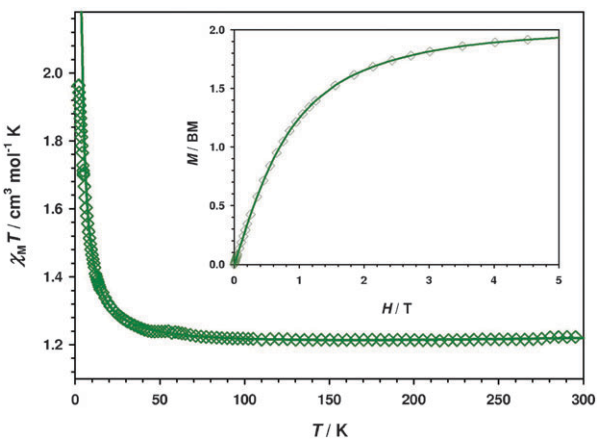

Fig. 13 A $\chi_M T$ *vs.* T plot for **5** (□) under applied fields of 1 T ($T > 15$ K), 0.1 T ($T < 15$ K); (□) experimental data; (—) best-fit curve through eqns (4) and (5). The inset shows the magnetization *vs.* H plot for **5** at 2.0 K (the solid line is only an eye-guide).

most likely due to zero-field splitting effects. The assumption of a negligible exchange coupling between the nickel(II) ions across the extended 4,4′-bpy bridge allows us to consider the magnetic behaviour of **5** as corresponding to a two-dimensional quadratic arrangement of nickel(II) ions connected through *anti–syn* carboxylate bridges. Therefore, we can analyze the magnetic behaviour of **5** through a high-temperature series expansion derived from the two-dimensional Heisenberg model for an $S = 1$ manifold ferromagnet square lattice [eqns (4) and (5)]:[39]

$$\chi = [Ng^2\beta^2/(3kT)]X\left(1 + \sum_{n=1}^{8} A_n(X)K^n\right) \qquad (4)$$

where

$$A_n(X) = \sum_{i=1}^{n} a_i X^i;\ X = S(S+1) \text{ and } K = J/kT \qquad (5)$$

and N, g, β and k have their usual meanings. a_i are the coefficients for the square lattice and J is the intralayer magnetic coupling defined by the isotropic Hamiltonian

$$\hat{H} = -J\sum_i \hat{S}_i \cdot \hat{S}_{i+1}.$$

In this approach, the single-ion zero-field splitting of the Ni(II) ions is not considered, and only the high-temperature experimental data ($T > 15$ K) have been taken into account during the fitting procedure. The best-fit parameters are $J = +0.272(3)$ cm^{-1}, $g = 2.175(3)$ and $R = 4.7 \times 10^{-4}$. The nature and magnitude of the magnetic coupling between the nickel(II) ions through the *anti–syn* carboxylate bridge in **5** is in agreement with the results of a few magneto-structural studies with carboxylate-bridged nickel(II) complexes.[40]

Prior to the analysis and discussion of the magnetic data of **7** and **8**, we would like to briefly comment on the trend of the magnetic coupling between the paramagnetic centers of **1–5** through the *anti–syn* carboxylate pathway. The *anti–syn* carboxylate bridge with the apical-equatorial exchange pathways that occur in **1** and in other magneto-structurally characterized carboxylate (R-malonate)-bridged copper(II) compounds are known to mediate weak but significant ferromagnetic interactions (values of J covering the range from $+0.0049$ to $+1.8$ cm^{-1}), the accidental orthogonality between the two interacting magnetic orbitals [the magnetic orbital is the molecular orbital that defines the unpaired electron on each copper(II) ion] accounting for this ferromagnetic coupling.[4k,41] As the number of unpaired electrons on the metal ion increases [two for Ni(II) (**5**), three for Co(II) (**4**), and five for Mn(III) (**3**) and Fe(III) (**2**)], the possibility of a net overlap between the magnetic orbitals increases (and then to an increase of the antiferromagnetic terms), leading to a decrease of the ferromagnetic coupling (in the case of **5**) and even to an overall antiferromagnetic interaction (in the cases of **4**, **3** and **2**).

The thermal dependence of the $\chi_M T$ product [χ_M being the magnetic susceptibility per copper(II) ion] for complexes **7** and **8** are plotted in Fig. 14. The values of $\chi_M T$ at room temperature are 0.42 and 0.41 cm^3 mol^{-1} K for **7** and **8**, respectively, and are as expected for a magnetically isolated spin doublet.

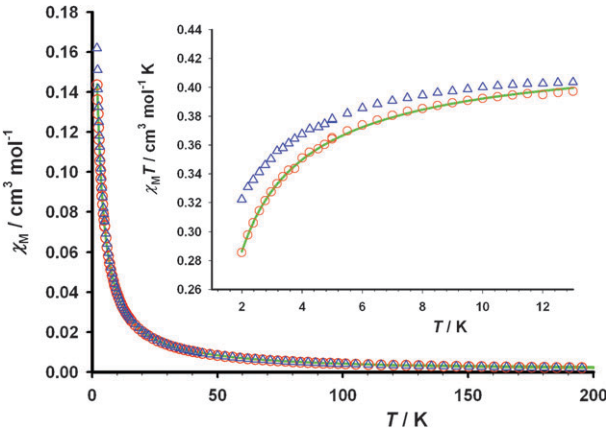

Fig. 14 $\chi_M T$ *vs.* T plot for **7** (△) and **8** (○) under applied magnetic fields of 1 T ($T > 15$ K), 0.1 T (15 K $> T >$ 5 K) and 0.02 T ($T < 5$ K) for **7**, and 1 T ($T > 15$ K) and 0.1 T ($T < 15$ K) for **8**; (○) experimental data; (—) best-fit curve through eqn (6) (see text). The inset shows detail of the low temperature $\chi_M T$ *vs.* T dependence.

Upon cooling, $\chi_M T$ remains almost constant up to 40 K and then smoothly decreases to reach values of 0.32 (**7**) and 0.28 (**8**) cm^3 mol^{-1} K at 2.0 K. Both plots are indicative of an overall weak antiferromagnetic coupling between the copper(II) ions.

Complex **8** is a uniform copper(II) chain where the extended O–C–C–C–O methyl malonate skeleton constitutes the intrachain exchange pathway that connects equatorial positions of adjacent copper(II) ions, the metal–metal separation being *ca.* 6.77 Å. Consequently, its magnetic data were analyzed by the numerical expression derived by Bonner and Fisher for a uniform chain of copper(II) ions with $J < 0$ [eqn (6)][40]

$$\chi_M = \frac{Ng^2\beta^2}{kT}\frac{0.25 + 0.074875x + 0.075235x^2}{1 + 0.9931x + 0.172135x^2 + 0.757825x^3} \qquad (6)$$

with $x = J/kT$ and the Hamiltonian being defined by $\hat{H} = -J\sum_i \hat{S}_i \cdot \hat{S}_{i+1}$. The best-fit parameters using non-linear regression analysis are $J = -1.38(2)$ cm^{-1}, $g = 2.135(1)$ and $R = 3.3 \times 10^{-5}$. The calculated curve matches well with the experimental data over the whole temperature range (see the inset of Fig. 14). Concerning the nature of the magnetic coupling through this uncommon exchange pathway in **8**, a previous report on the complex {[Cu(2,2′-bpy)(H$_2$O)][Cu(2,2′-bpy)(mal)(H$_2$O)]}(ClO$_4$)$_2$, where the same O–C–C–C–O (malonate) bridging pathway connecting equatorial positions at the copper atoms is involved,[4s] evidenced an antiferromagnetic coupling of -4.2 cm^{-1}, a value that was also supported by DFT-type calculations. The somewhat weaker antiferromagnetic coupling in **8** with respect to that in the 2,2′-bpy-containing complex is due to the different conformation of the Cu–O–C–C–C–O–Cu motif (*anti–syn* in **8** *vs.* *anti–anti* in the previous compound).

Analysis of the magnetic data of **7** is more complicated because of the presence of three possible exchange pathways: (i) the *anti–syn* carboxylate(Memal) concerning Cu(1)···Cu(2) and Cu(1)···Cu(2g), with copper–copper distances of 5.6430(9) and 5.6248(9) Å (equatorial–axial), respectively, (ii) the more extended O–C–C–C–O methylmalonate skeleton

connecting Cu(2) and Cu(2g) separated by 9.2487(11) Å (axial–axial), and finally (iii) the bis-monodentate 4,4′-bpy building a square grid of copper(II) ions separated by 11.2198(12) Å (equatorial–equatorial) [Cu(1)···Cu(1m); m = $-x + 1$, $y + \frac{1}{2}$, $-z + 1$)]. On the basis of the previous studies, weak ferromagnetic interactions are expected through the (i) pathway, whereas weak but antiferromagnetic couplings are also expected across the two latter pathways. In the absence of an appropriate model to analyze the magnetic data of **7**, one can conclude that the overall antiferromagnetic behaviour observed for this compound obeys to a larger contribution of the antiferromagnetic (ii) and (iii) exchange pathways *vs*. the ferromagnetic pathway represented by (i).

Conclusions

In this work, we have illustrated the ability of the methylmalonate ligand to form complexes with a variety of transition metal ions. Despite its flexibility, the Memal ligand forms reproducible robust structures with the 4,4′-bipyridine coligand and the Cu(II), Fe(III), Mn(II), Co(II), Ni(II) and Zn(II) ions. In these compounds, the 4,4′-bpy acts as pillar of an *anti–syn* carboxylate-bridged two-dimensional network, yielding a 3D [$4^4 6^6$]-**sqp** net. Weak but significant magnetic coupling occurs within these layers. Since the ferromagnetic coupling observed in the copper(II) complex comes from the accidental orthogonality, this interaction diminishes [in the case of Ni(II)] or even becomes antiferromagnetic [in the case of Co(II), Mn(II) and Fe(III)] when the number of unpaired electrons increases, and thus does the probability of overlap. The facility of the copper(II) ion to adopt different environments and the flexibility of the methylmalonate ligand to adopt various coordination modes lead to the formation of exotic structures like **7** and **8**, where different roles are played by the Memal group (a linear connector or part of a pillaring unit). Exploration of the coordination chemistry of these systems with changes in the coligand toward larger and bulkier groups to separate the layers, and toward small groups that can favour the magnetic interaction between layers, is in progress.

Acknowledgements

Financial support from the Spanish Ministerio de Educación y Ciencia through projects MAT2007-60660, CTQ2007-61690 and "Factoría de Cristalización, Consolider-Ingenio2010" CSD2006-0015, the Generalitat Valenciana (Grupos 03/197) and Agencia Canaria de Investigación, Innovación y Sociedad de la Información PIL2070901 are gratefully acknowledged. M. D. acknowledges a predoctoral FPU-AP2007-02435 fellowship from the Ministerio de Ciencia e Innovación (MICINN). J. P. also thanks CSD2006-0015 for a post-doctoral contract.

References

1 J. S. Miller and A. J. Epstein, *MRS Bull.*, 2000, **25**, 21.
2 B. Moulton and M. Zaworotko, *Chem. Rev.*, 2001, **101**, 1629.
3 G. R. Desiraju, *Crystal Engineering: The Design of Organic Solids*, Elsevier, Amsterdam, 1989.
4 Malonate containing Cu(II) complexes: (*a*) P. Gómez-Saiz, R. Gil-García, M. A. Maestro, F. J. Arnaiz, L. Lezama, T. Rojo, J. L. Pizarro, M. I. Arriortúa, M. González-Álvarez, J. Borrás, V. Diez-Gómez and J. García-Tojal, *Eur. J. Inorg. Chem.*, 2009, 373; (*b*) F. S. Delgado, F. Lahoz, F. Lloret, M. Julve and C. Ruiz-Pérez, *Cryst. Growth Des.*, 2008, **8**, 3219; (*c*) W.-L. Meng, G.-X. Liu, T. Okamura, H. Kawaguchi, Z.-H. Zhang, W.-Y. Sun and N. Ueyama, *Cryst. Growth Des.*, 2006, **6**, 2092; (*d*) F. S. Delgado, J. Sanchiz, C. Ruiz-Pérez, F. Lloret and M. Julve, *CrystEngComm*, 2004, **6**, 443; (*e*) F. S. Delgado, C. Ruiz-Pérez, J. Sanchiz, F. Lloret and M. Julve, *CrystEngComm*, 2006, **8**, 507; (*f*) F. S. Delgado, C. Ruiz-Pérez, J. Sanchiz, F. Lloret and M. Julve, *CrystEngComm*, 2006, **8**, 530; (*g*) S. Konar, S. Mukherjee, M. G. B. Drew, J. Ribas and N. R. Chaudhuri, *Inorg. Chem.*, 2003, **42**, 2545; (*h*) S. Sain, T. K. Maji, G. Mostafa, T.-H. Lu and N. R. Chaudhuri, *New J. Chem.*, 2003, **27**, 185; (*i*) F. S. Delgado, J. Sanchiz, C. Ruiz-Pérez, F. Lloret and M. Julve, *Inorg. Chem.*, 2003, **42**, 5938; (*j*) C. Ruiz-Pérez, Y. Rodríguez-Martín, M. Hernández-Molina, F. S. Delgado, J. Pasán, J. Sanchiz, F. Lloret and M. Julve, *Polyhedron*, 2003, **22**, 2111; (*k*) J. Pasán, F. S. Delgado, Y. Rodríguez-Martín, M. Hernández-Molina, C. Ruiz-Pérez, J. Sanchiz, F. Lloret and M. Julve, *Polyhedron*, 2003, **22**, 2143; (*l*) T.-F. Liu, H.-L. Sun, S. Gao, S.-W. Zhang and T.-Ch. Lau, *Inorg. Chem.*, 2003, **42**, 4792; (*m*) Y. Rodríguez-Martín, M. Hernández-Molina, F. S. Delgado, J. Pasán, C. Ruiz-Pérez, J. Sanchiz, F. Lloret and M. Julve, *CrystEngComm*, 2002, **4**, 440; (*n*) Y. Rodríguez-Martín, M. Hernández-Molina, F. S. Delgado, J. Pasán, C. Ruiz-Pérez, J. Sanchiz, F. Lloret and M. Julve, *CrystEngComm*, 2002, **4**, 522; (*o*) J. Sanchiz, Y. Rodríguez-Martín, C. Ruiz-Pérez, A. Mederos, F. Lloret and M. Julve, *New J. Chem.*, 2002, **26**, 1624; (*p*) Y. Rodríguez-Martín, J. Sanchiz, C. Ruiz-Pérez, F. Lloret and M. Julve, *CrystEngComm*, 2002, **4**, 631; (*q*) Y. Rodríguez-Martín, C. Ruiz-Pérez, J. Sanchiz, F. Lloret and M. Julve, *Inorg. Chim. Acta*, 2001, **318**, 159; (*r*) C. Ruiz-Pérez, J. Sanchiz, M. Hernández Molina, F. Lloret and M. Julve, *Inorg. Chem.*, 2000, **39**, 1363; (*s*) C. Ruiz-Pérez, M. Hernández-Molina, P. Lorenzo-Luis, F. Lloret, J. Cano and M. Julve, *Inorg. Chem.*, 2000, **39**, 3845; (*t*) Y. Rodríguez-Martín, C. Ruiz-Pérez, J. Sanchiz, F. Lloret and M. Julve, *Inorg. Chim. Acta*, 2001, **326**, 20; (*u*) D. Chattopadhyay, S. K. Chattopadhyay, P. R. Lowe, C. H. Schalwe, S. K. Mazumder, A. Rana and S. Ghosh, *J. Chem. Soc., Dalton Trans.*, 1993, 913.
5 Malonate containing Ni(II) and Co(II) complexes: (*a*) M. R. Montney, R. M. Suplowski and R. L. LaDuca, *Polyhedron*, 2008, **27**, 2997; (*b*) F. S. Delgado, M. Hernández-Molina, J. Sanchiz, C. Ruiz-Pérez, Y. Rodríguez-Martín, F. Lloret and M. Julve, *CrystEngComm*, 2004, **6**, 106; (*c*) F. S. Delgado, J. Sanchiz, C. Ruiz-Pérez, F. Lloret and M. Julve, *CrystEngComm*, 2003, **5**, 280; (*d*) S. Konar, P. S. Mukherjee, M. G. B. Drew, J. Ribas and N. R. Chaudhuri, *Inorg. Chem.*, 2003, **42**, 2545; (*e*) I. Gil de Muro, M. Insausti, L. Lezama, J. L. Pizarro, M. I. Arriortua and T. Rojo, *Eur. J. Inorg. Chem.*, 1999, 935.
6 Malonate containing Mn(II) complexes: (*a*) A. Cuevas, C. Kremer, L. Suescun, S. Russi, A. W. Mombru, F. Llorert, M. Julvem and J. Faus, *Dalton Trans.*, 2007, 5305; (*b*) S. C. Manna, E. Zangrando, M. G. B. Drew, J. Ribas and N. R. Chaudhuri, *Eur. J. Inorg. Chem.*, 2006, 481; (*c*) Y. Rodríguez-Martín, M. Hernández-Molina, J. Sanchiz, C. Ruiz-Pérez, F. Lloret and M. Julve, *Dalton Trans.*, 2003, 2359; (*d*) T. K. Maji, S. Sain, G. Mostafa, T.-H. Lu, J. Ribas, M. Monfort and N. R. Chaudhuri, *Inorg. Chem.*, 2003, **42**, 709; (*e*) I. Gil de Muro, M. Insausti, L. Lezama, M. K. Urtiaga, M. I. Arriortua and T. Rojo, *J. Chem. Soc., Dalton Trans.*, 2000, 3360.
7 (*a*) M. O'Keeffe, *Chem. Soc. Rev.*, 2009, **38**, 1215; (*b*) D. J. Tranchemontagne, J. L. Mendoza-Cortés, M. O'Keeffe and O. M. Yaghi, *Chem. Soc. Rev.*, 2009, **38**, 1257; (*c*) C. N. R. Rao, S. Natarajan and R. Vaidhyanathan, *Angew. Chem., Int. Ed.*, 2004, **43**, 1466–1496.
8 (*a*) *Chem. Soc. Rev.*, 2009, **38** (Themed issue: Metal-Organic Frameworks, ed. J. R. Long and O. M. Yaghi); (*b*) B. Kesanli and W. Lin, *Coord. Chem. Rev.*, 2003, **246**(1–2), 305 (Structure, Properties and Applications of Inorganic Polymers); (*c*) O. M. Yaghi, M. O'Keeffe, N. W. Ockwig, H. K. Chae, M. Eddaoudi and J. Kim, *Nature*, 2003, **423**, 705; (*d*) S. L. James, *Chem. Soc. Rev.*, 2003, **32**, 276.
9 (*a*) J. Lu, C. Yu, T. Niu, T. Paliwala, G. Crisci, F. Somosa and A. J. Jacobson, *Inorg. Chem.*, 1998, **37**, 4637; (*b*) O. M. Yaghi, H. Li and T. L. Groy, *Inorg. Chem.*, 1997, **36**, 4292.

10 (*a*) K. Biradha, K. V. Domasevitch, B. Moulton, C. Seward and M. J. Zaworotko, *Chem. Commun*., 1999, 1327; (*b*) M. Fujita, Y. J. Kwon, S. Washizu and K. Ogura, *J. Am. Chem. Soc*., 1994, **116**, 1151; (*c*) L. Carlucci, G. Ciani and D. M. Proserpio, *New J. Chem*., 1998, **22**, 1319.

11 (*a*) L. R. MacGillivray, S. Subramaniam and M. J. Zaworotko, *J. Chem. Soc., Chem. Commun*., 1994, 1325; (*b*) A. J. Blake, N. R. Champness, S. S. M. Chung, W. S. Li and M. Schröder, *Chem. Commun*., 1997, 1005.

12 K. N. Power, T. L. Hennigar and M. J. Zaworotko, *Chem. Commun*., 1998, 595.

13 (*a*) B. F. Abrahams, B. F. Hoskins, R. Robson and D. A. Slizys, *CrystEngComm*, 2002, **4**, 478; (*b*) L. Carlucci, G. Ciani, D. M. Proserpio and A. Sironi, *Angew. Chem., Int. Ed. Engl*., 1995, **34**, 1895; (*c*) H. W. Roesky and M. Andruh, *Coord. Chem. Rev*., 2003, **236**, 91; (*d*) K. Biradha, M. Sarkar and L. Rajput, *Chem. Commun*., 2006, 4169.

14 Phmal containing complexes: (*a*) J. Pasán, J. Sanchiz, C. Ruiz-Pérez, J. Campo, F. Lloret and M. Julve, *Polyhedron*, 2010, *submitted*; (*b*) J. Pasán, J. Sanchiz, C. Ruiz-Pérez, J. Campo, F. Lloret and M. Julve, *Chem. Commun*., 2006, 2857; (*c*) J. Pasán, J. Sanchiz, C. Ruiz-Pérez, F. Lloret and M. Julve, *Inorg. Chem*., 2005, **44**, 7794; (*d*) J. Pasán, J. Sanchiz, C. Ruiz-Pérez, F. Lloret and M. Julve, *Eur. J. Inorg. Chem*., 2004, 4081; (*e*) J. Pasán, J. Sanchiz, C. Ruiz-Pérez, F. Lloret and M. Julve, *New J. Chem*., 2003, **27**, 1557.

15 Memal containing complexes: (*a*) J. Pasán, J. Sanchiz, F. Lloret, M. Julve and C. Ruiz-Pérez, *CrystEngComm*, 2007, **9**, 478; (*b*) C. Gkioni, A. K. Boudalis, Y. Sanakis and C. P. Raptopoulou, *Polyhedron*, 2007, **26**, 2536; (*c*) J. Pasán, J. Sanchiz, L. Cañadillas-Delgado, O. Fabelo, M. Déniz, F. Lloret, M. Julve and C. Ruiz-Pérez, *Polyhedron*, 2009, **28**, 1802; (*d*) C. M. Perkins, N. J. Rose and R. E. Stenkamp, *Inorg. Chim. Acta*, 1990, **172**, 119.

16 R. L. Carlin, *Magnetochemsitry*, Springer-Verlag, Berlin Heidelberg, Germany, 1986.

17 *SADABS, version 2.03*, Bruker AXS Inc., Madison, WI, 2000.

18 G. M. Sheldrick, *Acta Crystallogr., Sect. A: Found. Crystallogr*., 2008, **64**, 112–122.

19 *WINGX*: L. J. Farrugia, *J. Appl. Crystallogr*., 1999, **32**, 837.

20 M. Nardelli, *J. Appl. Crystallogr*., 1995, **28**, 659.

21 *DIAMOND 2.1d*, Crystal Impact GbR, K. Brandenburg & H. Putz GbR, Postfach 1251, D-53002 Bonn, Germany, 2000.

22 H. D. Flack, *Acta Crystallogr., Sect. A: Found. Crystallogr*., 1983, **39**, 876.

23 R. Baldomá, M. Monfort, J. Ribas, X. Solans and M. A. Maestro, 2006, **45**, 1415.

24 M. O'Keeffe, M. A. Peskov, S. J. Ramsden and O. M. Yaghi, *Acc. Chem. Res*., 2008, **41**, 1782–1789.

25 C. Janiak, *J. Chem. Soc., Dalton Trans*., 2000, 3885.

26 M. Nishio, *CrystEngComm*, 2004, **6**(27), 130–158.

27 E. I. Stiefel and G. F. Brown, *Inorg. Chem*., 1972, **11**, 434.

28 (*a*) M. Julve, M. Verdaguer, J. Faus, F. Tinti, J. Moratal, A. Monge and E. Gutiérrez-Puebla, *Inorg. Chem*., 1987, **26**, 3520; (*b*) S. Subramanian and M. J. Zaworotko, *Angew. Chem., Int. Ed. Engl*., 1995, **34**, 2127; (*c*) M. X. Li, G. Y. Xie, Y. D. Gu, J. Chen and P. J. Zheng, *Polyhedron*, 1995, **14**, 1235; (*d*) J. Lu, T. Paliwala, S. C. Lim, C. Yu, T. Niu and A. J. Jacobson, *Inorg. Chem*., 1997, **36**, 923; (*e*) K. N. Power, T. L. Hennigar and M. J. Zaworotko, *New J. Chem*., 1998, **22**, 177; (*f*) H. Y. Shen, D. Z. Liao, Z. H. Jiang, S. P. Yan, B. W. Sun, G. L. Wang, X. K. Yao and H. G. Wang, *Polyhedron*, 1998, **17**, 1953; (*g*) M. L. Tong, B. H. Ye, J. W. Cai, X. M. Chen and S. W. Ng, *Inorg. Chem*., 1998, **37**, 2645; (*h*) J. Lu, C. Yu, T. Niu, T. Paliwala, G. Crisci, F. Somosa and A. J. Jacobson, *Inorg. Chem*., 1998, **37**, 4637; (*i*) M. A. Lawandy, X. Huang, R. J. Wang, J. Li, J. Y. Lu, T. Yuen and C. L. Lin, *Inorg. Chem*., 1999, **38**, 5410; (*j*) Y. S. Zhang, G. D. Enright, S. R. Breeze and S. Wang, *New J. Chem*., 1999, **23**, 6256; (*k*) M. L. Tong, H. J. Chen and X. M. Chen, *Inorg. Chem*., 2000, **39**, 2235; (*l*) J. Gao, X. Y. Xu, M. Y. Wang, Q. L. Liu and H. B. Song, *J. Coord. Chem*., 2005, **58**, 1351; (*m*) X. D. Wang, M. Liang, L. C. Li, Z. H. Jiang, D. Z. Liao, S. P. Yang and P. Cheng, *Struct. Chem*., 2007, **18**, 5; (*n*) O. Sereda and H. Stoeckli-Evans, *Acta Crystallogr., Sect. C: Cryst. Struct. Commun*., 2008, **64**, m221.

29 (*a*) S. Noro, S. Kitagawa, M. Kondo and K. Seki, *Angew. Chem., Int. Ed*., 2000, **39**, 2081; (*b*) S. Noro, R. Kitaura, M. Kondo, S. Kitagawa, T. Ishii, H. Matsuzaka and M. Yamashita, *J. Am. Chem. Soc*., 2002, **124**, 2568.

30 A. W. Addison, T. N. Rao, J. Reedijk, J. van Rijn and G. C. Verschoor, *J. Chem. Soc., Dalton Trans*., 1984, 1349.

31 (*a*) Y. Zhang, J. Li, J. Chen, Q. Su, W. Deng, M. Nishiura, T. Imamoto, X. Wu and Q. Wang, *Inorg. Chem*., 2000, **39**, 2330; (*b*) A. D. Burrows, R. W. Harrington, M. F. Mahon and C. E. Price, *J. Chem. Soc., Dalton Trans*., 2000, 3845.

32 (*a*) M. E Lines, *J. Phys. Chem. Solids*, 1970, **31**, 101; (*b*) M. E. Lines, *J. Chem. Phys*., 1971, **55**, 2977.

33 (*a*) S. Domínguez, A. Mederos, P. Gili, A. Rancel, A. E. Rivero, F. Brito, F. Lloret, X. Solans, C. Ruiz-Pérez, M. L. Rodríguez and I. Brito, *Inorg. Chim. Acta*, 1997, **255**, 367; (*b*) A. Rodríguez, H. Sakiyama, N. Masciocchi, S. Galli, N. Gálvez, F. Lloret and E. Colacio, *Inorg. Chem*., 2005, **44**, 8399.

34 (*a*) B. N. Figgis, M. Gerloch, J. Lewis, F. E. Mabbs and G. A. Webb, *J. Chem. Soc. A*, 1968, 2086; (*b*) M. Gerloch and P. N. Quested, *J. Chem. Soc. A*, 1971, 3729; (*c*) J. M. Herrera, A. Bleuzen, Y. Dromzée, M. Julve, F. Lloret and M. Verdaguer, *Inorg. Chem*., 2003, **42**, 7052; (*d*) D. Maspoch, N. Domingo, D. Ruiz-Molina, K. Wurst, J. M. Hernández, G. Vaughan, C. Rovira, F. Lloret, J. Tejada and J. Veciana, *Inorg. Chem*., 2007, **46**, 1627.

35 (*a*) M. E. Lines, *J. Chem. Phys*., 1971, **55**, 2977; (*b*) G. De Munno, M. Julve, F. Lloret, J. Faus and A. Caneschi, *J. Chem. Soc., Dalton Trans*., 1994, 1175; (*c*) G. De Munno, T. Poerio, M. Julve, F. Lloret and G. Viau, *New J. Chem*., 1998, **22**, 299; (*d*) A. K. Sharma, F. Lloret and R. Mukherjee, *Inorg. Chem*., 2007, **46**, 5128.

36 (*a*) C. Ruiz-Pérez, J. Sanchiz, M. Hernández-Molina, F. Lloret and M. Julve, *Inorg. Chim. Acta*, 2000, **298**, 202; (*b*) D. Ghoshal, G. Mostafa, T. K. Maji, E. Zangrando, T.-H. Lu, J. Ribas and N. R. Chaudhuri, *New J. Chem*., 2004, **28**, 1204; (*c*) F. S. Delgado, M. Hernández-Molina, J. Sanchiz, C. Ruiz-Pérez, Y. Rodríguez-Martín, T. López, F. Lloret and M. Julve, *CrystEngComm*, 2004, **6**, 106; (*d*) O. Fabelo, J. Pasán, L. Cañadillas-Delgado, F. S. Delgado, F. Lloret, M. Julve and C. Ruiz-Pérez, *Inorg. Chem*., 2008, **47**, 8053.

37 (*a*) O. Fabelo, J. Pasán, L. Cañadillas-Delgado, F. S. Delgado, C. Yuste, F. Lloret, M. Julve and C. Ruiz-Pérez, *CrystEngComm*, 2009, **11**, 2169; (*b*) O. Fabelo, J. Pasán, F. Lloret, M. Julve and C. Ruiz-Pérez, *CrystEngComm*, 2007, **9**, 815–827; (*c*) M. Julve, M. Verdaguer, J. Faus, F. Tinti, J. Moratal, A. Monge and E. Gutiérrez-Puebla, *Inorg. Chem*., 1987, **26**, 3520.

38 F. Lloret, M. Julve, J. Cano, R. Ruiz and E. Pardo, *Inorg. Chim. Acta*, 2008, **361**, 3432–3445.

39 (*a*) M. S. Haddad, D. N. Hendrickson, J. P. Cannady, R. S. Drago and D. S. Bieksza, *J. Am. Chem. Soc*., 1979, **101**, 898; (*b*) M. Julve, M. Verdaguer, J. Faus, F. Tinti, J. Moratal, A. Monge and E. Gutiérrez-Puebla, *Inorg. Chem*., 1987, **26**, 3520; (*c*) I. Castro, J. Sletten, M. L. Calatayud, M. Julve, J. Cano, F. Lloret and A. Caneschi, *Inorg. Chem*., 1995, **34**, 4903.

40 W. E. Estes, D. P. Gavel, W. E. Hatfield and D. Hodgson, *Inorg. Chem*., 1978, **17**, 1415.

41 (*a*) A. Rodríguez-Fortea, P. Alemany, S. Álvarez and E. Ruiz, *Chem.–Eur. J*., 2001, **7**, 627; (*b*) E. Colacio, M. Ghazi, R. Kivekäs and J. M. Moreno, *Inorg. Chem*., 2000, **39**, 2882; (*c*) R. L. Carling, K. Kopinga, O. Kahn and M. Verdaguer, *Inorg. Chem*., 1986, **25**, 1786; (*d*) K. K. Nanda, A. W. Addison, E. Sinn and L. K. Thompson, *Inorg. Chem*., 1996, **35**, 5966; (*e*) E. Colacio, J. M. Domínguez-Vera, R. Kivekäs, J. M. Moreno, A. Romerosa and J. Ruiz, *Inorg. Chim. Acta*, 1993, **212**, 115; (*f*) E. Colacio, J. P. Costes, R. Kivekäs, J. P. Laurent and J. Ruiz, *Inorg. Chem*., 1990, **29**, 4240; (*g*) E. Colacio, J. M. Domínguez-Vera, J. P. Costes, R. Kivekäs, J. P. Laurent, J. Ruiz and M. Sundberg, *Inorg. Chem*., 1992, **31**, 774; (*h*) M. Murugesu, R. Clérac, B. Pilawa, A. Mandel, C. E. Anson and A. K. Powell, *Inorg. Chim. Acta*, 2002, **337**, 328; (*i*) D. K. Towle, S. K. Hoffmann, W. E. Hatfield, P. Singh and P. Chaudhuri, *Inorg. Chem*., 1988, **27**, 394.